

PARAMETER ESTIMATION BASED MODELS
OF WATER SOURCE HEAT PUMPS

By

HUI JIN

Bachelor of Science
Shanghai Jiaotong University
Shanghai, China
1992

Master of Science
Shanghai Jiaotong University
Shanghai, China
1995

Submitted to the Faculty of the
Graduate College of the
Oklahoma State University
in partial fulfillment for
the requirements for
the degree of
DOCTOR OF PHILOSOPHY
December 2002

PARAMETER ESTIMATION BASED MODELS
OF WATER SLOURCE HEAT PUMPS

Thesis Approved:

Thesis Adviser

Dean of the Graduate College

ACKNOWLEDGEMENTS

I wish to express my sincere appreciation to all of the people who helped me to accomplish this dissertation.

First and foremost, I wish to thank my advisor, Dr. Jeffrey D. Spitler. His expertise and respected reputation in the HVAC field allowed for the funding of many projects and the opportunity for me to adopt knowledge and experience in modeling of building thermal systems. I am grateful for your constructive guidance and leadership.

I would like to extend my gratitude to the members of my doctoral committee, Dr. D. E. Fisher, Dr. A. J. Ghajar and Dr. Jim Bose for their committed service and support, ideas and suggestions that helped improve my work significantly.

Thanks also to Dr. Marvin Smith who provided input and experimental data regarding the water-to-water heat pump model validation. Fred Schroeder, Development Engineer, with the Division of Engineering Technology also provided valuable information and help on the portions of the water-to-water heat pump experimental data.

I wish to deliver special credit to Dr. Fisher and David Eldridge for their generous assistance on the experimental validation of the water-to-air heat pump model.

It's hard to find any words to express the thanks to my parents, Zhixue Jin and Lingdi Jiang and my wife, Pony for their love and understanding along the way.

Last, but not least, I would like to thank my colleagues in B-10, ATRC, MAE Research Lab and Electronics Lab, both here and gone, namely, Dr. Cenk Yavuzturk,

Andrew Chiasson, Mahadevan Ramamoorthy, Xiaobing Liu, Dongyi Xiao and Chanvit, for their ideas and precious help in a direct or indirect way.

Support of the U.S. Department of Energy under the grant numbers DE-FG48-97R810627 and DE-FG48-94R689416, and of the Federal Highway Administration under grant number DTFH61-99-X-00067 is gratefully acknowledged.

TABLE OF CONTENTS

<i>Chapter</i>	<i>Page</i>
1. Introduction.....	1
2. Literature Review	4
2.1. Heat Pump and Chiller Models.....	4
2.1.1. Equation-fit Models	4
2.1.1.1. Allen and Hamilton Model	4
2.1.1.2. Hamilton and Miller Model	7
2.1.1.3. Stoecker and Jones Model	9
2.1.2. Models Falling Between the Two Extremes.....	12
2.1.2.1. Stefanuk et al. Model	12
2.1.2.2. Domanski and Didion Model.....	14
2.1.2.3. Cecchini and Marchal Model.....	18
2.1.2.4. Bourdouxhe, et al. Model.....	22
2.1.2.5. Gordon and Ng Model	27
2.1.2.6. Parise Model	29
2.1.2.7. Fischer and Rice Model	32
2.1.2.8. The Comparison by Damasceno, et al.	44
2.1.2.9. Shelton and Weber Model	44
2.1.2.10. Greyvenstein Model.....	45
2.1.2.11. Dabiri Model.....	47
2.1.2.12. Ouazia and Snelson’s Model	49
2.1.2.13. Krakow and Lin’s Model.....	50
2.2. Modeling of Heat Pump Components.....	54
2.2.1. Analysis of Heat Transfer between Moist Air and Cold Surface by McElgin and Wiley.....	54
2.2.2. Analysis of Air Side Heat Transfer in Finned Tube Heat Exchangers by Webb	56
2.2.3. Experimental Results of Chilled-Water Cooling Coils Operating at Low Water Velocities by Mirth et al	57
2.2.4. Comparison of Methods of Modeling the Air Side Heat and Mass Transfer in Chilled-Water Cooling Coils by Mirth and Ramadhyani	58
2.2.5. Cooling Coil Model of Braun, et al.	59
2.2.6. Parameter Estimation Technique of Rabehl, et al.	65
2.2.7. Reciprocating Compressor Model of Popovic and Shapiro.....	67
2.2.8. ARI Standard 540-99	70
2.2.9. Ganesh et al. Coil Model	71

<i>Chapter</i>	<i>Page</i>
2.2.10. Hassab and Kamal Coil Model	85
2.2.11. Khan Coil Model.....	91
2.2.12. Expansion Device	95
2.2.13. Modeling of Rotary Compressors.....	96
2.2.13.1. Analysis of Chu, et al.....	96
2.2.13.2. Analysis of Wakabayashi, et al.....	97
2.2.13.3. Simulation Model for Fixed Vane Rotary Compressor of Gyberg and Nissen.....	98
2.2.13.4. Model of Rotary Compressor to Simulate its Transient Behavior by Yanagisawa et al.	98
2.2.13.5. An Analytical Model for Rotary Air Compressor by Huang.....	99
2.2.13.6. Dynamic Analysis of a Rotary Compressor by Padhy.....	100
2.2.13.7. A Simulation Model of an A/C Rotary Vane Compressor by Takeshita	100
2.2.13.8. A Computer Simulation of a Rotary Compressor by Ooi and Wong	101
2.2.13.9. Heat Transfer Analysis of a Rolling-Piston Rotary Compressor by Padhy and Dwivedi.....	101
2.2.13.10. A review of Rotary Compressor Design Evolution for Heat Pump Application by Barratt and Murzinski	102
2.3. Literature Review Summary	102
3. Objectives and Scope	104
4. A Parameter Estimation Based Model for Water-To-Water Heat Pumps	107
4.1. System Description	117
4.2. Compressor Model.....	118
4.3. Condenser and Evaporator Models.....	123
4.4. Expansion Device	125
4.5. Parameter Estimation Procedure.....	125
4.6. Model Implementation.....	133
4.7. Treatment of Extreme Operating Conditions.....	136
4.8. Model Validation	136
4.9. Discussion of Parameter Selections	142
4.10. Comparison to an Equation-fit Model	146
4.11. Conclusion for Water-to-Water Heat Pump Model	151
5. A Parameter Estimation Based Model for Water-to-Air Heat Pumps.....	153
5.1. System Description	154
5.2. Compressor Model.....	155
5.3. Sensible Heat Exchanger Model.....	156
5.4. Direct Expansion Cooling Coil Model	157
5.4.1. Total Heat Transfer Rate.....	160
5.4.2. Split of Total Heat Transfer Rate.....	163
5.5. Expansion Device	166
5.6. Parameter Estimation Procedure.....	167

<i>Chapter</i>	<i>Page</i>
5.6.1. Objective function #1 for external heat transfer coefficient $h_{c,o}A_o$	169
5.6.2. Objective function #2 for the remaining parameters	171
5.7. Model Implementation.....	175
5.8. Treatment of Extreme Operating Conditions.....	179
5.9. Model Validation	179
5.10. Prediction of Dry Coil Condition using Wet Coil Parameters.....	188
5.11. Conclusion for Water-to-Air Heat Pump Model and Recommendations for Future Work	191
6. Extensions for the Parameter Estimation Based Heat Pump Models.....	195
6.1. Modeling of Scroll Compressor.....	195
6.1.1. Model	195
6.1.2. Algorithm.....	204
6.1.3. Validation.....	209
6.2. Modeling of Rotary Compressor	212
6.3. Modeling of Heat Pump Performance with Anti-Freeze	218
6.3.1. Derivation of Antifreeze Degradation Factor	219
6.3.2. Volumetric Flow-Dependent Heat Exchanger Model	222
6.3.3. Volumetric Flow-Dependent Heat Exchanger Model	227
6.4. Conclusions and Recommendations	233
7. Water-to-Water Heat Pump Model Validation	235
7.1. Background and a Brief Description of Experimental Apparatus	235
7.2. The Hydronic Heating System.....	238
7.2.1. Water-to-Water Heat Pump	238
7.2.2. Water Circulation Pumps.....	239
7.2.3. Ground Loop Heat Exchanger	239
7.2.4. Medium-Scale Bridge Deck.....	240
7.3. Instrumentation	240
7.3.1. Fluid Flow Rates.....	241
7.3.2. Inlet and Outlet Fluid Temperatures	241
7.3.3. Power Consumption.....	242
7.3.4. Data Acquisition and Logging.....	242
7.4. Physical Properties of the Propylene Glycol Solution.....	243
7.5. A Preliminary Analysis of Experimental Uncertainty	246
7.6. The Manufacturer's Catalog Data for the Heat Pump	249
7.7. Parameter Estimation and a Comparison Between Model Prediction and Catalog Data.....	251
7.8. Model Uncertainty	254
7.9. Experiments	258
7.10. Dec. 11 2000 Experiment	259
7.10.1. Experimental Uncertainty	260
7.10.2. Energy Imbalance	260

<i>Chapter</i>	<i>Page</i>
7.10.3. A Comparison of Model Prediction to the Experimental Data.....	263
7.11. Dec. 12, 2000 Experiment	268
7.12. Dec. 30, 2001 Experiment	271
7.12.1. Experimental Uncertainty	272
7.12.2. Energy Imbalance	273
7.12.3. A Comparison of Model Prediction to the Experimental Data.....	274
7.13. Summary	279
8. Water-to-Air Heat Pump Model Validation.....	281
8.1. Background and a Brief Description of Experimental Apparatus	281
8.2. The Heating and Air Conditioning System.....	283
8.2.1. Water-to-Air Heat Pump.....	283
8.2.2. Humidifier	284
8.2.3. Booster Fan	285
8.3. Instrumentation	285
8.3.1. Air Flow Rate.....	285
8.3.2. Return and Supply Air Dry Bulb Temperatures	287
8.3.3. Return Air Dew Point Temperature	288
8.3.4. Condensate.....	289
8.3.5. Water Flow Rate	290
8.3.6. Inlet and Outlet Water Temperatures.....	290
8.3.7. Power Consumption.....	291
8.3.8. Data Acquisition and Logging	291
8.4. Experimental Uncertainty	292
8.5. The Manufacturer’s Catalog Data for the Heat Pump	293
8.6. Parameter Estimation and a Comparison Between Model Prediction and Catalog Data	298
8.7. Model Uncertainty	305
8.8. Experiment in Heating Mode.....	308
8.8.1. Experimental Uncertainty	308
8.8.2. Energy Imbalance	309
8.8.3. A Comparison of Model Prediction to the Experimental Data.....	310
8.9. Experiment in Cooling Mode.....	315
8.9.1. Experimental Uncertainty	315
8.9.2. Energy Imbalance	317
8.9.3. Parameter Estimation Based on Experimental Data	318
8.9.4. A Comparison of Model Prediction to the Experimental Data.....	320
8.10. Summary	324
9. Conclusions and Recommendations.....	325
9.1. Conclusions.....	325
9.2. Recommendations.....	329
References.....	333

APPENDIX A - Sensitivity Analysis of the Water-to-Water Heat Pump Model....	345
APPENDIX B - Calibration of the Instrumentation for the Water-to-Air Heat Pump Experiment	354

LIST OF TABLES

<i>Table</i>	<i>Page</i>
2.1. Interpretation of Accuracy of Performance Predictions	44
4.1. Literature Review Summary for Heat Pump & Chiller Models	116
4.2. Range of Water Flow Rates and Entering Water Temperatures.....	134
4.3. RMS Errors of the Simulations for 4 Sets of Catalog Data	137
4.4. Comparison of the Search Results of the Objective Function	145
4.5. The Comparison of the Parameter Estimation Results for Heat Pump A in Cooling and Heating Modes	146
4.6. The Comparison of the Relative Error of Power Consumption Simulated by Parameter Estimation and Equation-fit Models	150
4.7. The Comparison of the Relative Error of Heating Capacity Simulated by Parameter Estimation and Equation-fit Models	151
5.1. A List of the HP's used for Model Verification	181
5.2. Range of Flow Rates and Temperatures (IP units)	181
5.3. Range of Flow Rates and Temperatures (SI units)	181
6.1. A Comparison of the Model Prediction RMS Errors.....	212
6.2. Parameter Estimation Results for the Trane Water-to-Air Heat Pump Model GSUJ 018 (Heating)	228
6.3. RMS Errors of Model Prediction Compared with Catalog Data (Trane GSUJ & WPVJ 018 Water-to-Air Heat Pump)	229
7.1. Heating Capacity Data for Model WP120	239
7.2. FHP WP 120 Catalog Data (IP Units)	250

<i>Table</i>	<i>Page</i>
7.3. FHP WP 120 Catalog Data (SI Units)	251
7.4. Parameter Estimation Results for the FHP Water-to-Water Heat Pump Model WP120	252
7.5. RMS Errors of the Simulations for the Catalog Data	254
7.6. Mean of Errors and Standard Deviation	256
7.7. Average Temperature Differences and Power Consumption used to Compute the Relative Uncertainties	260
7.8. Derived Uncertainties of Heat Transfer Rate and Power Consumption	260
7.9. Energy Imbalance with Estimated Uncertainties (12/11/2000)	263
7.10. Average Heat Transfer Rates and Power Consumption (19:00 –24:00).....	266
7.11. Average Temperature Differences and Power Consumption used to Compute the Relative Uncertainties	273
7.12. Derived Uncertainties of Heat Transfer Rate and Power Consumption	273
7.13. Energy Imbalance with Estimated Uncertainties (12/30/2001)	274
7.14. RMS Errors between Model Prediction and Experimental Data	279
8.1. RMS Errors between Model Prediction and Experimental Data	293
8.2. FHP GT018 Catalog Data for Cooling Mode (SI Units)	295
8.3. GT018 Catalog Data for Heating Mode (IP Units).....	297
8.4. GT018 Catalog Data for Heating Mode (SI Units).....	297
8.5. Parameter Estimation Results for the FHP Water-to-Air Heat Pump Model GT018 – Cooling Mode	298
8.6. Parameter Estimation Results for the FHP Water-to-Air Heat Pump Model GT018 – Heating Mode.....	299
8.7. RMS Errors of the Simulations for the Catalog Data	302
8.8. RMS Errors of the Simulations for the Catalog Data	304

<i>Table</i>	<i>Page</i>
8.9. Mean of Errors and Standard Deviation (Cooling).....	306
8.10. Mean of Errors and Standard Deviation (Heating).....	306
8.11. Estimated Model Uncertainty Based on Normal Distribution (Cooling Mode)....	306
8.12. Estimated Model Uncertainty Based on Normal Distribution (Heating Mode)	307
8.13. Total Model Uncertainty (Cooling Mode).....	307
8.14. Total Model Uncertainty (Heating Mode).....	307
8.15. Average Temperature Differences and Power Consumption used to Compute the Relative Uncertainties.....	308
8.16. Experimental Uncertainties of Heat Transfer Rate and Power Consumption	309
8.17. Energy Imbalance with Estimated Uncertainties.....	310
8.18. Average Heat Transfer Rates and Power Consumption	313
8.19. Uncertainty of Load Side Sensible Heat Transfer Rate.....	315
8.20. Uncertainty of Latent Heat Transfer Rate.....	316
8.21. Uncertainty of Source Side Heat Transfer Rate.....	316
8.22. Heat Pump Energy Imbalance	317
8.23. Energy Imbalance with Estimated Uncertainties (Data Point #1).....	318
8.24. Parameter Estimation Results for the FHP Water-to-Air Heat Pump Model GT018 – Cooling Mode	319
8.25. Parameter Estimation Results for the FHP Water-to-Air Heat Pump Model GT018 – Cooling Mode	320

LIST OF FIGURES

<i>Figure</i>	<i>Page</i>
2.1. Water chiller conceptual experiment	6
2.2. Inlet and outlet variables of a single fluid general component at steady-state conditions.....	8
2.3. Information-flow diagram for simulation the complete vapor-compression system	12
2.4. Temperature profile of the counter-flow concentric tube condenser.....	13
2.5. Thermodynamic compression cycle	21
2.6. Temperature-entropy diagram for the simulated heat pump.....	49
2.7. Schematic of a counter-flow cooling tower	62
2.8. Schematic of cooling and dehumidifying coil	74
2.9. Schematic of simple HVAC system	83
2.10. Schematic for counter flow cooling coil control volume.....	91
4.1. Basic heat pump configuration	117
4.2. Schematic indicator diagram for a reciprocating compressor.....	119
4.3. Pressure-enthalpy diagram for the refrigeration cycle.....	124
4.4. Flow diagram for parameter estimation computer program	132
4.5. Information flow chart for model implementation	133
4.6. Flow diagram for model implementation computer program.....	135
4.7. Calculated cooling capacity vs catalog cooling capacity (heat pump B).....	138
4.8. Calculated power vs catalog power (heat pump B)	138

<i>Figure</i>	<i>Page</i>
4.9. Calculated heating capacity vs catalog heating capacity (heat pump A).....	139
4.10. Calculated power vs catalog power (heat pump A).....	139
4.11. Calculated cooling capacity vs catalog cooling capacity (heat pump A)	140
4.12. Calculated power vs catalog power (heat pump A).....	140
4.13. Calculated heating capacity vs catalog heating capacity (heat pump C).....	141
4.14. Calculated power vs catalog power (heat pump C)	141
4.15. Calculated heating capacity vs catalog heating capacity using equation-fit (heat pump C)	149
4.16. Calculated power vs catalog power using equation-fit (heat pump C).....	149
5.1. Schematic of a water-to-air heat pump	153
5.2. Basic water-to-air heat pump configuration (cooling operation).....	155
5.3. Schematic of a counter-flow direct expansion coil.....	158
5.4. Flow diagram for parameter estimation computer program (#1).....	171
5.5. Flow diagram for parameter estimation computer program (#2).....	174
5.6. Information flow chart for model implementation	176
5.7. Flow diagram for model implementation computer program.....	178
5.8. Calculated total cooling capacity vs. catalog total cooling capacity (heat pump #1 all points)	183
5.9. Calculated total cooling capacity vs. catalog total cooling capacity (heat pump #1 32 points)	183
5.10. Calculated sensible cooling capacity vs. catalog sensible cooling capacity (heat pump #1 all points)	184
5.11. Calculated sensible cooling capacity vs. catalog sensible cooling capacity (heat pump #1 32 points)	184

<i>Figure</i>	<i>Page</i>
5.12. Calculated latent cooling capacity vs. catalog latent cooling capacity (heat pump #1 all points)	185
5.13. Calculated latent cooling capacity vs. catalog latent cooling capacity (heat pump #1 32 points)	185
5.14. Calculated heat rejection vs. catalog heat rejection (heat pump #1 all points).....	186
5.15. Calculated heat rejection vs. catalog heat rejection (heat pump #1 32 points).....	186
5.16. Calculated power consumption vs. catalog power consumption (heat pump #1 all points).....	187
5.17. Calculated power Consumption vs. catalog power consumption (heat pump #1 32 points)	187
5.18. Latent heat factor vs. wet bulb temperature (low dry bulb temp).....	189
5.19. Latent heat factor vs. wet bulb temperature (medium dry bulb temp).....	190
5.20. Latent heat factor vs. wet bulb temperature (high dry bulb temp).....	190
6.1. Scroll compression process.....	197
6.2. Thermodynamic cycle of a scroll compressor under design condition.....	199
6.3. Thermodynamic cycle of a scroll compressor with over-compression loss	200
6.4. Thermodynamic cycle of a scroll compressor with under -compression loss	201
6.5. Calculated heating capacity vs catalog heating capacity (Hypothetical reciprocating compressor).....	210
6.6. Calculated power vs catalog power (Hypothetical reciprocating compressor)	210
6.7. Calculated heating capacity vs catalog heating capacity (Scroll compressor)	211
6.8. Calculated power vs catalog power (Scroll compressor).....	211
6.9. Rotary compressor -- rolling piston type (ASHRAE handbook of HVAC systems and equipment)	215
6.10. Thermodynamic cycle of a rotary compressor.....	216

<i>Figure</i>	<i>Page</i>
6.11. Degradation factor for propylene glycol/water mixture by percent volume.....	222
6.12. Calculated heating capacity vs catalog heating capacity	228
6.13. Calculated power vs catalog power	229
6.14. Evaporator overall heat transfer resistance (Trane GSUJ 018 water-to-air heat pump).....	230
6.15. Heating capacity correction factor with varying flow rates (Trane GSUJ 018 water-to-air heat pump).....	232
6.16. Heating capacity correction factor with varying entering fluid temperatures (Trane GSUJ water-to-air heat pump).....	232
7.1. System schematic of the water-to-water heat pump experiment	237
7.2. Water-to-water heat pump in the instrumentation building.....	238
7.3. Density of aqueous solution of propylene glycol (42% by weight).....	244
7.4. Specific heat of aqueous solution of propylene glycol (42% by weight)	245
7.5. Thermal conductivity of aqueous solution of propylene glycol (42% by weight) ..	245
7.6. Dynamic viscosity of aqueous solution of propylene glycol (42% by weight)	246
7.7. Calculated heating capacity vs catalog heating capacity	253
7.8. Calculated extracted heat vs catalog extracted heat.....	253
7.9. Calculated power vs catalog power	254
7.10. Error Distribution.....	256
7.11. Heat pump load/source side flow rates	259
7.12. Heat pump energy imbalance (12/11/00).....	262
7.13. Heat pump model validation in heating mode: load side entering/leaving fluid temp	264
7.14. Heat pump model validation in heating mode: source side entering/leaving fluid temp	264

<i>Figure</i>	<i>Page</i>
7.15. Heat pump model validation in heating mode: power input.....	265
7.16. Heat pump model validation in heating mode: heating capacity percentage error between model and experiment	266
7.17. Heat pump model validation in heating mode: heating of extraction percentage error between model and experiment	267
7.18. Heat pump model validation in heating mode: power consumption percentage error between model and experiment	267
7.19. Heat pump load/source side flow rates	268
7.20. Heat pump model validation in heating mode: load side entering/leaving fluid temp	270
7.21. Heat pump model validation in heating mode: source side entering/leaving fluid temp.....	270
7.22. Heat pump model validation in heating mode: power input.....	271
7.23. Heat pump load/source side flow rates	272
7.24. Heat pump energy imbalance.....	273
7.25. Heat pump model validation in heating mode: load side entering/leaving fluid temp	275
7.26. Heat pump model validation in heating mode: source side entering/leaving fluid temp.....	275
7.27. Heat pump model validation in heating mode: power input.....	276
7.28. Heat pump model validation in heating mode: heating capacity percentage error between model and experiment	278
7.29. Heat pump model validation in heating mode: heating of extraction percentage error between model and experiment	278
7.30. Heat pump model validation in heating mode: power consumption percentage error between model and experiment	279
8.1. System schematic of the water-to-air heat pump experiment.....	282

<i>Figure</i>	<i>Page</i>
8.2. Front side of the tested water-to-air heat pump	284
8.3. Nozzle without throat taps ($L = D = 5$).....	286
8.4. Lay-out of the thermocouples on the screen used to measure the inlet and outlet air temperatures.....	287
8.5. Calculated total cooling capacity vs catalog total cooling capacity	300
8.6. Calculated sensible cooling capacity vs catalog sensible cooling capacity	301
8.7. Calculated latent cooling capacity vs catalog latent cooling capacity.....	301
8.8. Calculated heat rejection vs catalog heat rejection	302
8.9. Calculated power vs catalog power	302
8.10. Calculated heating capacity vs catalog heating capacity	303
8.11. Calculated extracted heating vs catalog extracted capacity	304
8.12. Calculated power vs catalog power	304
8.13. Heat pump energy balance (heating)	309
8.14. Heat pump model validation in heating mode: source side entering/leaving water temp.....	311
8.15. Heat pump model validation in heating mode: load side entering/leaving air temp	311
8.16. Heat pump model validation in heating mode: power consumption	312
8.17. Heat pump model validation in heating mode: heating capacity percentage error between model and experiment	313
8.18. Heat pump model validation in heating mode: heating extraction percentage error between model and experiment	314
8.19. Heat pump model validation in heating mode: power consumption percentage error between model and experiment	314
8.20. Calculated total cooling capacity vs experimental total cooling capacity	321

<i>Figure</i>	<i>Page</i>
8.21. Calculated sensible cooling capacity vs experimental sensible cooling capacity..	322
8.22. Calculated latent cooling capacity vs experimental latent cooling capacity.....	322
8.23. Calculated heat rejection vs experimental heat rejection.....	323
8.24. Calculated power consumption vs experimental power consumption.....	323

NOMENCLATURE

Symbols

A_w	=	wetted airside surface area on which moisture is condensing, m ² or ft ²
C	=	clearance factor
C_s	=	specific heat of saturated air, J/(kg-K) or Btu/(lbm-F)
C_p	=	specific heat, J/(kg-K) or Btu/(lbm-F)
f_g	=	sensible heat transfer coefficient through air film, W/(m ² -K) or Btu/(hr-°F-ft ²)
h	=	enthalpy of air vapor mixture per pound of dry air evaluated at the main stream temperature, kJ/kg or Btu/lbm
$h_{c,o}A_o$	=	outside surface heat transfer coefficient, kW/K or Btu/(hr-F)
h	=	enthalpy, J/kg or Btu/lbm
h_s	=	enthalpy of air vapor mixture per pound of dry air evaluated at the surface temperature, kJ/kg or Btu/lbm
H_T	=	total heat loss by total weight of air flowing over wetted surface, kW or Btu/hr
\dot{m}	=	mass flow rate, kg/s or lbm/hr
NTU	=	number of transfer units
P	=	pressure, Pa or psia
PD	=	piston displacement, m ³ /s or CFM
\dot{Q}	=	heat transfer rate, W or Btu/hr
s	=	humid specific heat of air vapor mixture, kJ/(kg dry air - °C) or Btu/(lbm dry air - °F)
S	=	thermostat signal
T	=	temperature, °C , °F or °K
UA	=	heat transfer coefficient, W/K or Btu/(hr-F)
$(UA)_i$	=	inside surface heat transfer coefficient, kW/K or Btu/(hr-F)
V	=	specific volume, m ³ /kg or ft ³ /lbm
w	=	humidity ratio, kg/kg dry air

\dot{W}	=	compressor power input, W or Btu/hr
γ	=	isentropic exponent
η	=	loss factor used to define the electro-mechanical loss that is supposed to be proportional to the theoretical power
ε	=	thermal effectiveness of heat exchanger
ΔT_{sh}	=	superheat, °C or °F
ΔP	=	pressure drop across suction or discharge valve, Pa or psia

Subscripts

a	=	air
A	=	A state point in refrigeration cycle
B	=	B state point in refrigeration cycle
c	=	condensing state
com	=	compressor
cat	=	catalog data
dis	=	discharge state
dry	=	dry condition
e	=	evaporating state
hi	=	high pressure cut-off
i	=	inlet condition, i th calculated result or inside surface
in	=	compressor inlet state
L	=	load side
lo	=	low pressure cut-off
$loss$	=	constant part of the electro-mechanical power losses
o	=	outlet condition or outside surface

<i>out</i>	=	compressor outlet state
<i>r</i>	=	refrigerant
<i>s</i>	=	saturated state or outside surface
<i>S</i>	=	source side
<i>sen</i>	=	sensible
<i>t</i>	=	Theoretical power
<i>suc</i>	=	suction state
<i>w</i>	=	water
<i>wet</i>	=	wet condition

1. Introduction

Reciprocating vapor compression heat pumps and chillers have been the target of a number of simulation models. Hamilton and Miller (1990) presented a classification scheme for air conditioning equipment with two extremes. At one end of the spectrum are equation-fit models, called “functional fit” models by Hamilton and Miller, which treat the system as a black box and fit the system performance to one or a few large equations. At the other end are deterministic models, called “first principle” models by Hamilton and Miller, which are detailed models based on applying thermodynamic laws and fundamental heat and mass transfer relations to individual components.

Many of the models found in the literature might actually fall between the two extremes, although the detailed deterministic models often apply equation-fitting for some of the components. For example, in the reciprocating chiller model proposed by Bourdouxhe, et al. (1994), the chiller was modeled as an assembly of several simplified components. Each component (e.g., compressor, evaporator, condenser, expansion device) is modeled with a detailed deterministic approach. The parameters describing the detailed physical geometry and operation of each component are then adjusted (i.e., in an equation-fit procedure) to reproduce the behavior of the actual unit as accurately as possible. The model of Bourdouxhe, et al. requires more details for each component than what is usually available from the manufacturers’ catalogs. This type of model is most suitable for users that have access to internally measured data (e.g., in Bourdouxhe’s

model, condensing and evaporating temperatures and subcooling and superheating temperature differences) from the chiller or heat pump.

The alternative approach, equation-fitting, alleviates the need for internally measured data and usually maintains better fidelity to the catalog data. It also usually requires less computational time. These models are most suitable for users that only have access to catalog data. These models would not be useful for someone attempting to design a heat pump or chiller by modifying or replacing internal components. Especially troublesome for some applications, extrapolation of the model may lead to unrealistic results.

It is desirable to have a model that only requires catalog data, but allows extrapolation beyond the catalog data. In the authors' experience, this model has been extremely useful for modeling of ground source heat pumps in novel applications where the fluid temperatures occasionally go beyond the catalog data. It is also useful in simulations that are part of a ground loop sizing procedure. In this application, it often happens that the temperatures are well beyond the catalog data. Even though the ultimate outcome is that the ground loop heat exchanger size will be adjusted to bring the temperatures within reasonable limits, it is helpful to have a model that does not catastrophically fail when the temperatures are too high or too low.

The model presented in this report uses deterministic models of each heat pump component. Each of the fundamental equations describing the system components may

have one or more parameters, which are estimated simultaneously using catalog data only; no other experimental data are required. The parameter estimation is done with a multi-variable optimization method. Once the parameters have been estimated, the heat pump model may be used as part of a multi-component system simulation.

This modeling approach has the advantage of not requiring experimental data beyond what are published in the manufacturer's catalog. Yet, its predictions are of similar or better accuracy than previously published deterministic models that required additional experimental data. Unlike the equation-fit models, the model domain may be extended beyond the catalog data without catastrophic failure in the prediction.

2. Literature Review

2.1. Heat Pump and Chiller Models

Simulation models of vapor-compression refrigeration and air-conditioning systems such as heat pumps and chillers have been the topic of numerous papers. The models can generally be classified in terms of the degree of complexity and empiricism. A review of the literature reveals a few limitations on existing models. For the more deterministic models, there is a gap between what data are provided by manufacturers' catalogs and what data the simulation models require. For equation-fit models, the valid application is limited to the manufacturer-supplied data range and conditions.

2.1.1. Equation-fit Models

2.1.1.1. Allen and Hamilton Model

Allen and Hamilton (1983) proposed a steady state reciprocating water chiller model which can be used for full and part load performance evaluation. This model is a typical equation-fit model. Other modeling algorithms employing the equation-fit approach are similar to this method. This water chiller model was a model of the complete system and did not consist of individual component models or involve internal pressures and temperatures. Although basic equations governing the steady state water chiller operation can be obtained by applying basic physical laws to the systems, the author eliminated the internal variables by utilizing the functional relationships among variables and examining typical water chiller performance data. For example, evaporator

cooling load was expressed by a polynomial in terms of evaporator water and condenser water temperatures in which several constant coefficients were actually fitted by a regression approach:

$$QE = B_1 \cdot TE_2 + B_2 \cdot TC_2 + B_3 \cdot TE_2 \cdot TC_2 + B_4 \cdot TE_2^2 + B_5 \cdot TC_2^2 + B_6 \quad (2.1)$$

where QE = evaporator cooling load, kW or Btu/hr

TE_2 = evaporator leaving water temperature, °C or °F

TC_2 = condenser leaving water temperature. °C or °F

Similarly, the compressor energy balance can also be expressed by the following polynomial equation,

$$P = B_7 \cdot TE_2 + B_8 \cdot TC_2 + B_9 \cdot TE_2 \cdot TC_2 + B_{10} \cdot TE_2^2 + B_{11} \cdot TC_2^2 + B_{12} \quad (2.2)$$

where P = compressor power, kW or Btu/hr

TE_2 = evaporator leaving water temperature, °C or °F

TC_2 = condenser leaving water temperature, °C or °F

The evaporator water energy balance, condenser water energy balance and the simple thermal balance for the whole system are expressed respectively as:

$$QE = ME \cdot C_p \cdot (TE_1 - TE_2) \quad (2.3)$$

$$QC = MC \cdot C_p \cdot (TC_2 - TC_1) \quad (2.4)$$

$$QC = QE + P \quad (2.5)$$

where ME = evaporator water mass flow rate, kg/s or lbm/hr

C_p = water specific heat, kJ/(kg-K) or Btu/(lbm-°F)

QC = condenser heat rejection rate, kW or Btu/hr

MC = condenser water mass flow rate, kg/s or lbm/hr

TC_1 = condenser entering water temperature, °C or °F

TE_1 = evaporator entering water temperature, °C or °F

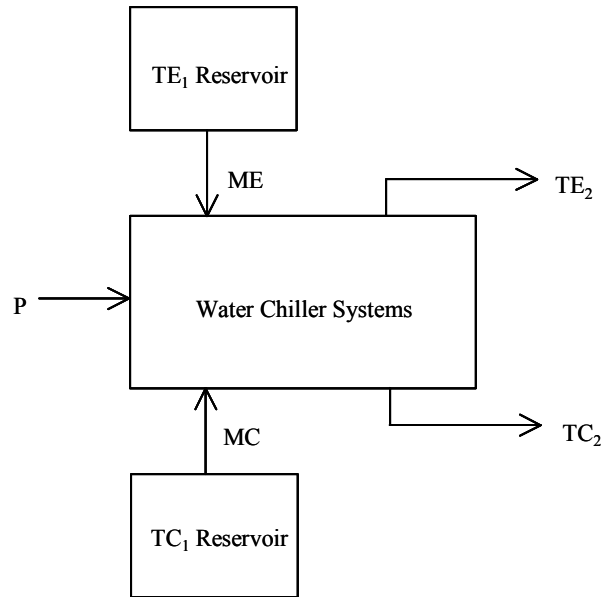


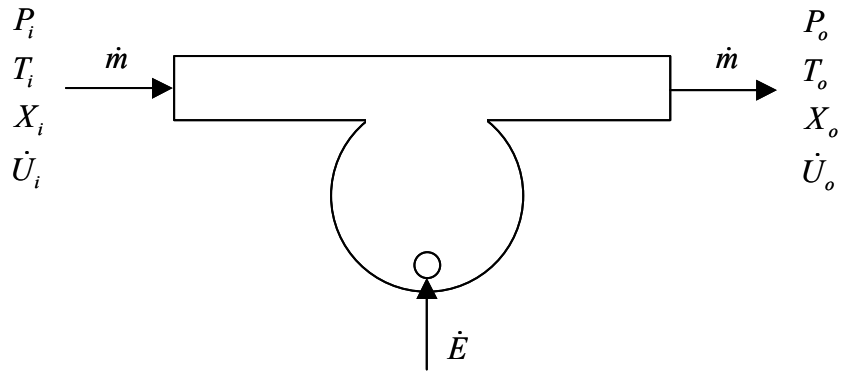
Figure 2.1. Water chiller conceptual experiment

The constant coefficients in above equations B_1 - B_{12} are to be determined. The physical significance of the model, consisting of five equations and nine variables, can be envisioned in a conceptual experiment which is described in the paper. Given a water chiller, Figure 2.1, a reservoir of chilled water at TE_1 with a mass flow rate of ME , and a

reservoir of cooling water at TC_1 with a mass flow rate of MC , then the five system equations can be solved for energy rates QE , P and QC and leaving temperatures TE_2 and TC_2 .

2.1.1.2. Hamilton and Miller Model

The Allen and Hamilton (1983) model utilizes overall system data, e.g. entering and leaving water temperatures and flow rates. In contrast, the model of Hamilton and Miller (1990) requires more detailed data, such as internal refrigerant pressures and temperatures. Hamilton and Miller (1990) developed this general steady state model by equation-fitting manufacturers' catalog data of the individual components, along with thermodynamic relationships. The model is capable of simulating the response of an air-conditioning system configuration for a variety of ambient and inside conditions. According to the author, any air conditioning system can be divided into components such as heat exchangers, fans, etc. It permits modeling a particular air conditioning system with the general usefulness of the simulation program. Several models of each component can be made and combined into a broad range of air conditioning systems using the concepts of mass and energy flow continuity and pressure-temperature compatibility at each component connection. The conceptual model of each component consists of an energy balance and a mass balance at steady state conditions yielding two rate equations for each component. Figure 2.2 illustrates the conceptual model for a general component operating at steady state conditions.



$$\begin{aligned} \dot{E} &= f_1(P_i, T_i, X_i, P_o, T_o, X_o) \\ \dot{m} &= f_2(P_i, T_i, X_i, P_o, T_o, X_o) \end{aligned}$$

where, \dot{E} = energy rate, kW or Btu/hr

\dot{m} = mass flow rate, kg/s or lbm/hr

P = pressure, kPa or psig

T = temperature, °C or °F

X = refrigerant quality

\dot{U} = energy flow rate, kW or Btu/hr

Figure 2.2. Inlet and outlet variables of a single fluid general component at steady-state conditions

The authors defined the model as a simulation tool for ‘air conditioning system’. Since air is the secondary working fluid in both evaporator and condenser, the equipment might be an air-to-air unit or split type air conditioner. The evaporator and condenser models include the air mass flow rates and the evaporator model accounts for the mass flow rate of the water condensing on the coil. Obviously, the mass flow rate of the water on condenser coils is zero.

The functional fit equations describing the individual component characteristics form a set of simultaneous algebraic rate equations describing the system performance. This model is actually a equation-fit model, but it established a model for each component individually by internal operating conditions, instead of treating the whole system as a black box. According to the author, in the general simulation developed in this work, each component model is primarily based on data available in manufacturers' catalogs. Similar to the deterministic model, those detailed component performance data are usually not readily available.

2.1.1.3. Stoecker and Jones Model

Stoecker and Jones (1982) present a vapor compression system simulation analysis. The purpose of the analysis is to predict the performance of the entire system when the characteristics of the individual components are known.

- *Reciprocating compressor*

The mathematical equations that represent the performance data is:

$$q_e = c_1 + c_2 t_e + c_3 t_e^2 + c_4 t_c + c_5 t_c^2 + c_6 t_e t_c + c_7 t_e^2 t_c + c_8 t_e t_c^2 + c_9 t_e^2 t_c^2 \quad (2.6)$$

and

$$P = d_1 + d_2 t_e + d_3 t_e^2 + d_4 t_c + d_5 t_c^2 + d_6 t_e t_c + d_7 t_e^2 t_c + d_8 t_e t_c^2 + d_9 t_e^2 t_c^2 \quad (2.7)$$

where q_e = refrigeration capacity, kW or Btu/hr

P = power required by compressor, kW or Btu/hr

t_e = evaporating temperature, °C or °F

t_c = condensing temperature, °C or °F

The constants applicable to Equations (2.6) and (2.7) for the compressor are determined by equation-fit procedures (i.e. the method of least squares). In addition to the refrigerating capacity and the power requirement of the compressor, another quantity of interest is the rate of heat rejection required at the condenser. The compressor catalogs show this quantity and usually it is simply the sum of the refrigerating and condensing temperatures.

$$q_c = q_e + P \quad (2.8)$$

where q_c is the rate of heat rejection at the condenser in kilowatts or Btu/hr.

- *Condenser performance*

The precise representation of the heat-transfer performance of a condenser can be quite complex, because the refrigerant vapor enters the condenser superheated and following the onset of condensation in the tube the fraction of liquid and vapor changes consequently through the condenser. A satisfactory representation of air-cooled condenser performance for most engineering calculations is available, however, through an assumption of a constant heat-exchanger effectiveness for the condenser, namely

$$q_c = F(t_c - t_{amb}) \quad (2.9)$$

where F = capacity per unit temperature difference, kW/K or Btu/(hr-°F)

t_{amb} = ambient temperature, °C or °F

- *Evaporator performance*

For subsequent mathematical simulation, an equation is needed to express the evaporator capacity. An adequate equation could originate from:

$$q_e = G(t_{wi} - t_e) \quad (2.10)$$

where t_{wi} = entering water temperature, °C or °F

G = proportionally factor, kW/K or Btu/(hr-°F)

The G value may be constant, or if the G value is not constant, as an approximation G can be proposed as a linear function of the temperature difference. For a particular case:

$$G = 6.0[1 + 0.046(t_{wi} - t_e)] \quad (2.11)$$

Thus,

$$q_e = 6.0[1 + 0.046(t_{wi} - t_e)](t_{wi} - t_e) \quad (2.12)$$

- *Simulation of complete system*

In the mathematical simulation, the three components can be simulated simultaneously.

The sequence of the calculation is shown by the information-flow diagram in Figure 2.3.

Similar to the model of Hamilton and Miller (1990), this model also requires more detailed data, such as internal refrigerant pressures and temperatures.

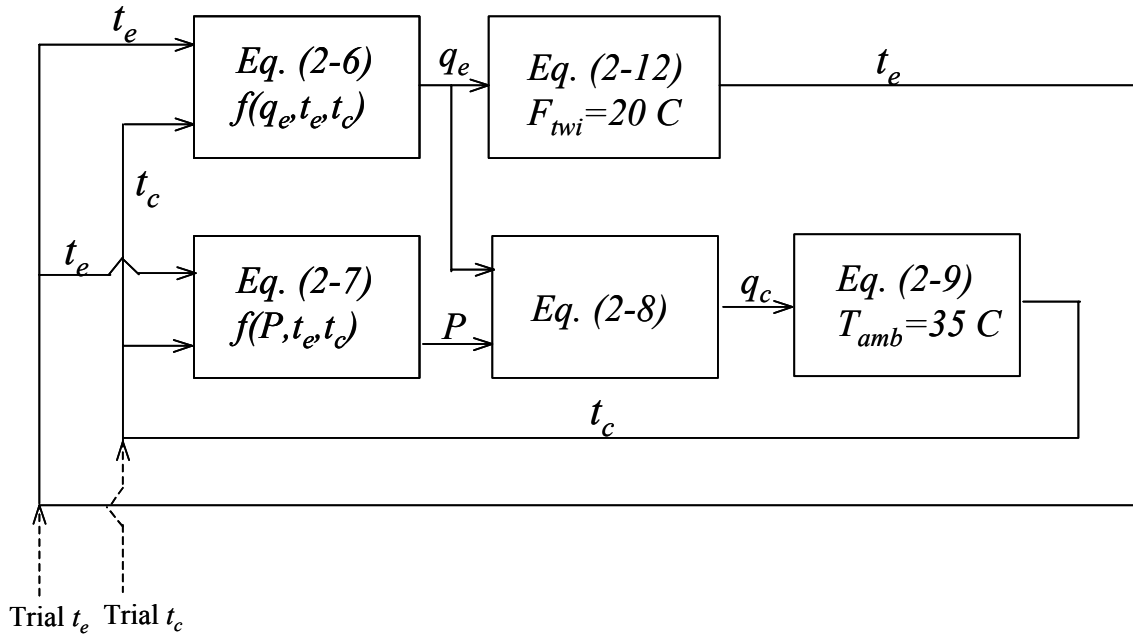


Figure 2.3. Information-flow diagram for simulation the complete vapor-compression system

2.1.2. Models Falling Between the Two Extremes

2.1.2.1. Stefanuk et al. Model

The superheat-controlled water-to-water heat pump model developed by Stefanuk, et al. (1992) may be the most detailed model presented to date. The authors claim “The model is derived entirely from the basic conservative laws of mass, energy, momentum and equations of state as well as fundamental correlations of heat transfer.” Each component is modeled to a very detailed level. For example, to simulate the real heat

transfer process in the condenser, the condenser itself is analyzed as three heat exchangers connected in series corresponding to the three phases of the refrigerant.

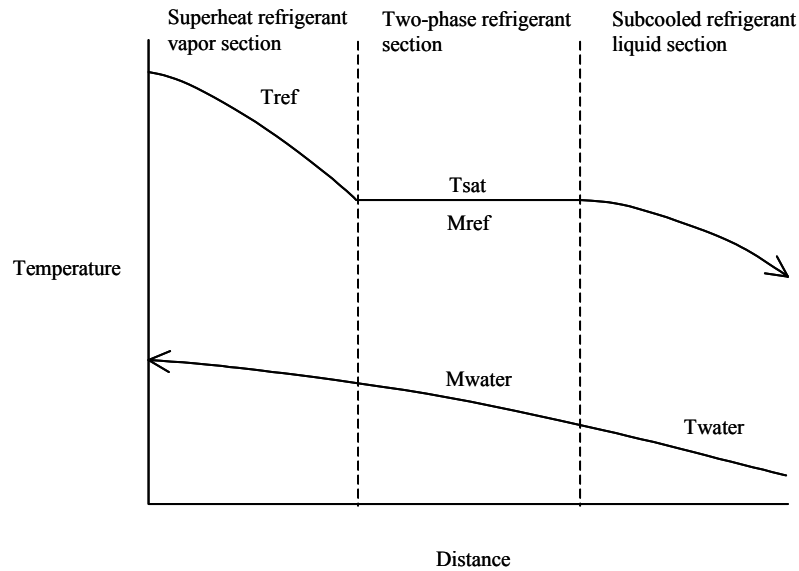


Figure 2.4. Temperature profile of the counter-flow concentric tube condenser

Values of the parameters that describe the behavior of the individual components are assumed to be available. For example, the parameters of the compressor are selected by “fitting the model to manufacturer-supplied performance curves that related mass flow rate and input electrical power to evaporation temperature and the compressor discharge pressure.” However, they are not normally available in the heat pump manufacturers’ catalogs. Comparisons between the experimental measurements and model predictions for the evaporating and condensing pressures, the heat transfer rates in the evaporator and the condenser, and the *COP* of the heat pump are given. Except a few points with errors beyond $\pm 10\%$, most of the results are generally acceptable. The predictions of the heat transfer rates in both heat exchangers are consistently too high. The authors explain that

the cause for this phenomenon is the overestimated predictions of heat transfer coefficients since heat transfer coefficients used in the model are only known to within $\pm 20\%$.

2.1.2.2. Domanski and Didion Model

Domanski and Didion (1984) developed a steady state model of an air-to-air heat pump having air to air heat exchangers, a capillary tube, and a reciprocating compressor. The basic assumption for the compressor simulation is that the highly dynamic compression process results in steady vapor flow condition through the compressor. Four internal locations are defined and refrigerant is considered to have uniform thermodynamic properties throughout the space assigned at the particular location. Heat transfer between these locations is governed by forced convection and is evaluated by expression based on the equation:

$$Nu \propto Re^{0.8} Pr^{0.333} \quad (2.13)$$

The refrigerant pressure drop within the compressor due to dynamic or friction effects is considered and evaluated based on the following expression respectively,

$$\Delta P \propto \frac{m^2}{\rho} \quad (2.14)$$

$$\Delta P \propto \mu^{0.2} \frac{m^{0.8}}{\rho} \quad (2.15)$$

where P = pressure, kPa or psia

m = refrigerant mass flow rate, kg/s or lbm/hr

ρ = density, kg/m³, or lbm/ft³

μ = dynamic viscosity, N-s/m² or centipoise

The process in the compressor is assumed to be polytropic for both compression and re-expansion, with the same polytropic index. The refrigerant enthalpy increment during polytropic compression is evaluated by the equation derived from the expression for isentropic and polytropic work of compression at the same compression pressure ratio,

$$\Delta i = \Delta i_s \frac{1}{\eta_p} \frac{R^{n-1/n} - 1}{R^{\gamma-1/\gamma} - 1} \quad (2.16)$$

where i = enthalpy, kJ/kg or Btu/lbm

$$\eta_p = \frac{\frac{\gamma-1}{n-1}}{n} \quad \text{polytropic efficiency}$$

R = compression pressure ratio

n = polytropic index

γ = isentropic index

subscript s = isentropic

Compressor energy balance is found iteratively by solving the equation,

$$E + m(i_3 - i_4) - Q_{can} = 0 \quad (2.17)$$

where E = electrical energy input rate to the compressor, kW or Btu/hr

m = refrigerant mass flow rate, kg/s or lbm/hr

i_3 = refrigerant enthalpy at compressor suction state, kJ/kg or Btu/lbm

i_4 = refrigerant enthalpy at compressor exhausting state, kJ/kg or Btu/lbm

Q_{can} = heat rejection rate from a compressor to ambient air, kW or Btu/hr

This model requires a variety of design parameters of the compressor and retains in some degree the complexity of the physical processes involved in describing the performance of a compressor, such as motor and mechanical efficiencies. The motor and mechanical efficiencies are related to the compressor motor and its interaction with the compressor. The polytropic and volumetric efficiencies are related to the processes occurring in the compressor cylinder. However, all of these parameters are based on the compressor manufacturer's one bench test.

Condenser and evaporator models are set up by a tube-by-tube simulation method which is based on an imaginary isolation of each finned tube from the coil assembly. The air to refrigerant heat transfer and refrigerant enthalpy change calculation are made on each tube independently. Heat transfer to/from each individual tube is calculated with the aid of the heat exchanger cross flow theory. Derived equations allow for consideration of two encountered cases: heat exchange between air and single-phase refrigeration

(temperature of both fluids change) and heat exchange between air and two-phase refrigerant (temperature of refrigerant is constant). For a tube in which change from one flow mode into another occurs, length of the tube with two-phase and single-phase is evaluated and heat transfer and pressure drop are evaluated accordingly. Overall heat transfer coefficient is calculated by the following equation,

$$U = \left[\frac{A_o}{h_i A_{p,i}} + \frac{A_o x_p}{A_{p,m} k_p} + \frac{1}{\frac{k}{\delta}} + \frac{1}{h_o \left(1 - \frac{A_f}{A_o} (1 - \phi) \right)} \right]^{-1} \quad (2.18)$$

where $h_o = h_c \cdot \left[1 + \frac{i_{fg,w} (w_a - w_w)}{C_{p,a} (T_a - T_w)} \right]$

U = overall heat transfer coefficient, kW/(m²-K) or Btu/(hr-ft²-°F)

A_o = pipe total outside surface area, m² or ft²

h_i = forced convection inside tube heat transfer coefficient,

kW/(m²-K) or Btu/(hr-ft²-°F)

$A_{p,i}$ = pipe inside surface area, m² or ft²

x_p = pipe wall thickness, m or ft

$A_{p,m}$ = pipe mean surface area, m² or ft²

k_p = thermal conductivity of pipe material, kW/(m-K) or Btu/(hr-ft-°F)

k = thermal conductivity of frost or water, kW/(m-K) or Btu/(hr-ft-°F)

δ = condensate (frost) layer thickness, m or ft

h_o = forced convection air side tube heat transfer coefficient modified for

the latent heat, kW/(m²-K) or Btu/(hr-ft²-°F)

A_f = fin surface area, m² or ft²

ϕ = fin efficiency

h_c = forced convection air side heat transfer coefficient, kW/(m²-K) or
Btu/(hr-ft²-°F)

$i_{fg,w}$ = latent heat of condensate of water, kJ/kg or Btu/lbm

w_a = air humidity ratio, kgv/kga, lbmv/lbma

w_w = humidity ratio of saturated air at water (frost) temperature,
kgv/kga, lbmv/lbma

$C_{p,a}$ = air specific heat at constant pressure, kJ/(kg-K) or Btu/(lbm-°F)

T_a = air temperature, °C or °F

T_w = temperature of water (frost) on a fin, °C or °F

2.1.2.3. Cecchini and Marchal Model

Cecchini and Marchal (1991) proposed a computer program for simulating refrigeration and air conditioning equipment of all types: air-to-air, air-to-water, water-to-water and water-to-air. The model presented did not describe in detail the operation of equipment but characterized it with a small number of parameters determined from the results of a few testing points. The author divided the simulation of a piece of equipment into two steps: evaluation of the characteristic parameters of the equipment; prediction of equipment performance at any operation conditions. The paper is presented by two parts.

In the first part the simulation model is described focusing on the refrigerant thermodynamic cycle, which is the same for all types of equipment. The heat exchanger laws for external fluids (water, air) at the evaporator and at the condenser, adapted to each type of equipment are also described. The second part deals with the comparison between computed results and experimental data.

The following simplifying assumptions are made:

- Steady-state operation (same mass flow of refrigerant in any part of the loop)
- Pressure drops neglected, except at the expansion valve
- Constant subcooling at the condenser outlet
- Constant superheating at the evaporator outlet

The thermodynamic cycle is presented in Figure 2.5.

Different components are simulated with the following set of equations:

- Compressor:
 - Enthalpy balance:

$$h_1 - h_3 = \frac{k}{k-1} \frac{P_v}{\rho_v} \left[\left(\frac{P_c}{P_v} \right)^{\frac{k-1}{k}} - 1 \right] \quad (2.19)$$

Where h_1 = compressor outlet refrigerant specific enthalpy, kJ/kg or Btu/lbm

h_3 = evaporator outlet refrigerant specific enthalpy, kJ/kg or Btu/lbm

k = polytropic exponent

P_v = refrigerant saturation pressure for evaporator, kPa or psia

P_c = refrigerant saturation pressure for condenser, kPa or psia

ρ_v = refrigerant saturation specific mass for evaporator, kg/m³ or lbm/ft³

- Volumetric balance:

$$q = \rho_v Q \left[1 - \tau \left(\left(\frac{P_c}{P_v} \right)^{1/k} - 1 \right) \right] \quad (2.20)$$

Where q = refrigerant mass flow rate, kg/s or lbm/hr

Q = swept volume, m³/s or CFM

τ = built-in volume ratio

These parameters (k , Q , τ) characterize the compressor size and compression irreversibility.

- Condenser
 - Thermal balance:

$$q(h_1 - h_2) = U_c (g_c - T_c) \quad (2.21)$$

Where U_c = thermal conductance on the refrigerant side, kW/K or Btu/(hr-°F)

q = refrigerant mass flow rate, kg/s or lbm/hr

h_1 = compressor outlet refrigerant specific enthalpy, kJ/kg or Btu/lbm

h_2 = condenser outlet refrigerant specific enthalpy, kJ/kg or Btu/lbm

\mathcal{G}_c = refrigerant saturation temperature for condenser, °C or °F

T_c = condenser mean surface temperature, °C or °F

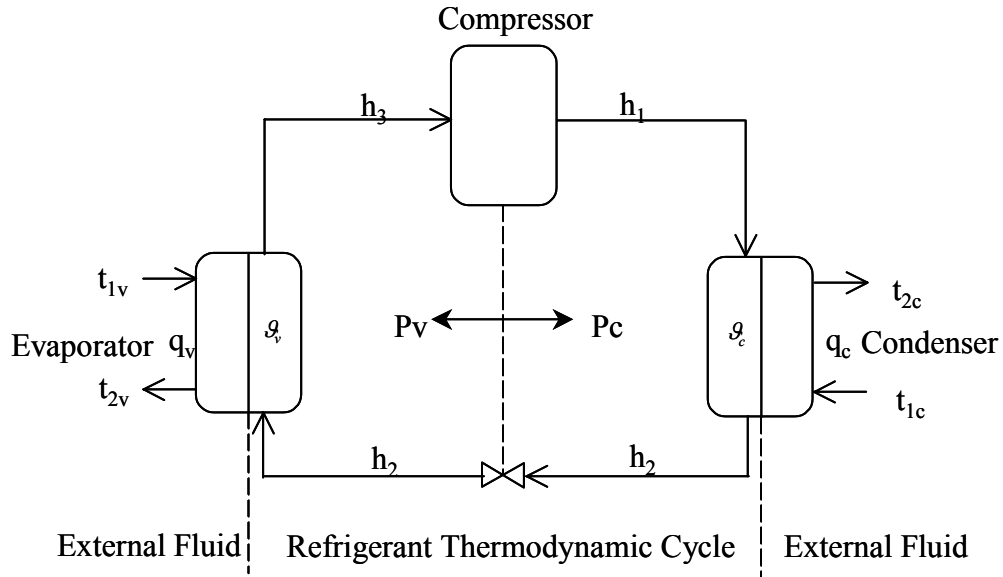


Figure 2.5. Thermodynamic compression cycle

- Evaporator
 - Thermal balance:

$$q(h_3 - h_2) = U_v(T_v - \mathcal{G}_v) \quad (2.22)$$

Where U_v = thermal conductance on the refrigerant side, kW/K or Btu/(hr-°F)

q = refrigerant mass flow rate, kg/s or lbm/hr

h_3 = evaporator outlet refrigerant specific enthalpy, kJ/kg or Btu/lbm

h_2 = condenser outlet refrigerant specific enthalpy, kJ/kg or Btu/lbm

g_v = refrigerant saturation temperature for evaporator, °C or °F

T_v = condenser mean surface temperature for evaporator, °C or °F

The author provided some correlations for thermal conductance on the refrigerant side. However, this model still requires detailed performance data for each component. The same disadvantages previously discussed appear again.

The model was first tested on three water-to-water heat pumps, ranging between 5 kW and 20 kW heat output. Predicted and measured capacities are compared on one piece of equipment. The uncertainty on capacity is about $\pm 5\%$. The results obtained with three air-to-air conditioners and one water-cooled air conditioner have an uncertainty of slightly higher than $\pm 10\%$.

2.1.2.4. Bourdouxhe, et al. Model

The quasi-static reciprocating chiller model developed by Bourdouxhe, et al. (1994) are characterized by the authors as being part of a toolkit “oriented towards simple solutions with a minimum number of parameters” and being somewhere between “curve-fitting, the traditional way to describe the input-output relationships, and deterministic modeling, which is an exhaustive description of the physical phenomena”. Their approach is to utilize a “conceptual schema” as a modeling technique to represent the unit as an assembly of classical and elementary components. The behavior of the each component is then modeled by a deterministic approach. This approach requires fewer

parameters and experimental data compared with the models developed previously. In the parameter identification procedure, the “available experimental data” such as the condensing and evaporating temperatures, the possible subcooling and superheating are required. Based on these experimental results, the parameters of the compressor are identified. Then the whole chiller is considered to identify the evaporator and condenser heat transfer coefficients. However, those experimental data are normally not available from manufacturers’ catalogs.

Both the condenser and the evaporator are represented as classical heat exchangers with water as secondary working fluid. No pressure drop is considered on the refrigerant side, and the refrigerant side is considered to be isothermal. The effectiveness model of such a heat exchanger is defined by the following relationship,

$$\varepsilon = 1 - e^{-NTU} \quad (2.23)$$

$$NTU = \frac{UA}{\dot{m}_w C_w} \quad (2.23a)$$

where ε = thermal effectiveness of heat exchanger

NTU = number of transfer units

UA = heat transfer coefficient, kW/K or Btu/(hr-°F)

\dot{m}_w = water mass flow rate, kg/s or lbm/hr

C_w = water specific heat, kJ/(kg-K) or Btu/(lbm-°F)

The heat transfer coefficient (UA) is prescribed to be independent of water flow rate thus remains constant during the simulation.

This is based on some idealized assumptions as follows:

- Isobaric aspiration of refrigerant into the cylinders,
- Isentropic compression,
- Isobaric expulsion of refrigerant from the cylinders, and
- Isentropic re-expansion of the refrigerant that remains in the clearance volume at the end of the expulsion process.

The refrigerant flow rate due to the re-expansion of the clearance volume is expressed by the following widely used equation,

$$\dot{V} = \dot{V}_s \left[1 + C_f - C_f \left(\frac{P_2}{P_1} \right)^{\frac{1}{\gamma}} \right] \quad (2.24)$$

where \dot{V} = volume flow rate, m³/s or CFM

\dot{V}_s = piston displacement of the compressor, m³/s or CFM

C_f = clearance factor

P_2 = compressor exhausting pressure, kPa or psia

P_1 = evaporator exhausting pressure, kPa or psia

γ = isentropic coefficient

The author describes the energy calculation of reciprocating chiller model in two parts: a parameter identification procedure and a simulation procedure. In the parameter identification procedure, the compressor is first considered separately from the whole heat pump. On the basis of some necessary experimental results, the data needed for each working point are:

- The condensing and evaporating temperature,
- The possible subcooling and superheat, and
- The refrigerating capacity and the power consumed by the compressor.

Four parameters chosen to represent the geometry and dynamics of the compressor are estimated. These are:

\dot{V}_s = piston displacement of the compressor, m³/s or CFM

C_f = clearance factor

W_{lo} = constant part of the electromechanical losses, kW or Btu/hr

α = loss factor used to define another electromechanical loss that is supposed to be proportional to the compressor's internal power

The isentropic compression power is:

$$\dot{W}_s = \epsilon_{vol} \dot{V}_s \frac{\gamma}{\gamma-1} p_1 \left[\left(\frac{p_2}{p_1} \right)^{\frac{\gamma-1}{\gamma}} - 1 \right] \quad (2.25)$$

where \dot{W}_s = isentropic compression power, kW or Btu/hr

\dot{V}_s = piston displacement of the compressor, m³/s or CFM

γ = isentropic coefficient

p_1 = pressure at the evaporator exhaust, kPa or psia

p_2 = pressure at the exhaust of the compressor cylinder, kPa or psia

$$\varepsilon_{vol} = 1 + C_f - C_f \left(\frac{p_2}{p_1} \right)^{\frac{1}{\gamma}}, \text{ volumetric effectiveness}$$

C_f = clearance factor

The electric power consumed by the compressor is:

$$\dot{W} = \dot{W}_{lo} + (1 + \alpha)\dot{W}_s \quad (2.26)$$

where \dot{W} = electrical power consumed by the compressor, kW or Btu/hr

\dot{W}_{lo} = constant part of the electromechanical losses, kW or Btu/hr

α = loss factor used to define another electromechanical loss that is
supposed to be proportional to the compressor's internal power

\dot{W}_s = isentropic compression power, kW or Btu/hr

When these parameters for the compressor are obtained, the whole chiller is considered. Here as mentioned above, only two parameters, the heat transfer coefficients (UA) for condenser and evaporator, shall be estimated. A set of coupled coefficients UA 's is extracted from a given domain of variation, and an objective function representing the relative error between experimental or catalog data and model calculation results for

power consumption and cooling capacity is set up. An exhaustive search method is employed to search for the optimal values of the heat transfer coefficients in this optimization problem.

2.1.2.5. Gordon and Ng Model

Gordon and Ng (1994) proposed a simple thermodynamic model for reciprocating chillers that they suggest might be valuable for diagnostic purposes. The model predicts the *COP* over a wide range of operation conditions from the inlet fluid temperatures and the cooling capacity, using three fitted parameters. The prediction of *COP* is remarkably good for a range of different chillers. However, the model doesn't predict the cooling capacity; it is required as an input.

The condenser and evaporator temperatures are approximated as constants, and expressed in terms of measured fluid temperatures and heat exchanger properties:

$$\begin{aligned}
 T_{cond} &= T_{cond}^{out} + \frac{Q_{evap} \left(1 + \frac{1}{COP}\right) [\exp(NTU_{cond}) - 1]}{(mC)_{cond}} \\
 &= T_{cond}^{in} + \frac{Q_{evap} \left(1 + \frac{1}{COP}\right) [1 - \exp(NTU_{cond})]}{(mC)_{cond}}
 \end{aligned} \tag{2.27}$$

$$\begin{aligned}
 T_{evap} &= T_{evap}^{in} - \frac{Q_{evap} [1 - \exp(-NTU_{evap})]}{(mC)_{evap}} \\
 &= T_{evap}^{out} - \frac{Q_{evap} [\exp(-NTU_{evap}) - 1]}{(mC)_{evap}}
 \end{aligned} \tag{2.28}$$

where ‘in’ and ‘out’ denote inlet and outlet fluid flows, ‘cond’ and ‘evap’ denote the condensing and evaporating temperatures, m is the mass flow rate, C is the coolant specific heat, and NTU is the number of transfer units.

Manufacturers’ catalog data usually report COP and Q_{evap} values at assorted values of condenser inlet temperature or condenser outlet temperature, and evaporator outlet temperature.

Recognizing that entropy S is a state function, and that chiller operation is cyclic, we have:

$$\Delta S = 0 = \frac{Q_{cond} - q_{cond}^{loss}}{T_{cond}} - \frac{Q_{evap} + q_{evap}^{loss}}{T_{evap}} \quad (2.29)$$

where q^{loss} refers to the losses from heat leaks, fluid friction, throttling, and desuperheating, and where heat transfer processes have been approximated as isothermal. If heat leaks are dominated by a linear heat transfer law and if isentropic throttling and desuperheating losses are not large and are typical of those in actual commercial chillers, then the function form of q^{loss} should be:

$$q_{cond}^{loss} = -A_0 + A_3 T_{cond} \quad (2.30)$$

$$q_{evap}^{loss} = -A_2 + A_4 T_{evap} \quad (2.31)$$

The constants A_0 , A_1 and A_2 characterize the irreversibilities of a particular chiller. The chiller can be characterized quantitatively by three parameters obtained by fitting the desired relation to sample measurements of the type reported in chiller catalogs. For particular realistic operating ranges of commercial chillers, not as a general cooling system description for all possible situations, a simplified expression for COP as a function of cooling rate, condenser inlet temperature, evaporator outlet temperature and other systems variables described above was obtained.

$$\frac{1}{COP} = -1 + \frac{T_{cond}^{in}}{T_{evap}^{out}} + \frac{-A_0 + A_1 T_{cond}^{in} - A_2 (T_{cond}^{in} / T_{evap}^{out})}{Q_{evap}} \quad (2.32)$$

It is demonstrated that the simple functional form predicted for the COP vs Q_{cool} curve agrees with actual performance data very well. The authors derived the equation for COP by actual experimental data with several constants to be determined and the accuracy of the predicted and measure COP was presented. However, the author did not provide any information about how to calculate the cooling capacity, power consumption and heat rejection by this model.

2.1.2.6. Parise Model

Parise (1986) developed a vapor compression heat pump simulation model to predict the overall performance of a system by employing a simple model for the

components of the heat pump cycle. Operating conditions, such as compressor speed, heat source and heat sink temperature, cooling and heating fluids flow rates, are entered as input data. Predetermined empirical parameters that characterize the components, such as the polytropic index of compression and heat exchangers' overall conductances, are also entered as input data. Predicted results were compared with experimental data. A typical application is presented at the end of the paper.

In the modeling of condenser and evaporator, these two heat exchangers are treated as having a constant overall heat transfer coefficient, based on the arithmetic overall temperature difference. For example, the heat transfer in the condenser is governed by the following equations,

$$\dot{Q}_{CD} = U_{CD} A_{CD} \left(\frac{T_2 + T_{CD}}{2} - \frac{T_{ci} + T_{co}}{2} \right) \quad (2.33)$$

$$\dot{Q}_{CD} = \dot{m}_F (h_2 - h_3) \quad (2.34)$$

$$\dot{Q}_{CD} = \dot{m}_c C_c (T_{co} - T_{ci}) \quad (2.35)$$

where \dot{Q}_{CD} = condenser heat transfer rate, kW or Btu/hr

U_{CD} = overall heat conductance of condenser, kW/(m²-°C)

A_{CD} = condenser heat transfer area, m² or ft²

T_2 = compressor outlet temperature, °C or °F

T_{CD} = condensing temperature, °C or °F

T_{ci} = condenser cooling fluid inlet temperature, °C or °F

T_{co} = condenser cooling fluid outlet temperature, °C or °F

\dot{m}_F = refrigerant mass flow rate, kg/s or lbm/hr

h_2 = refrigerant enthalpy at compressor outlet, kJ/kg or Btu/lbm

h_3 = refrigerant enthalpy at condenser outlet, kJ/kg or Btu/lbm

\dot{m}_c = condenser cooling fluid mass flow rate, kg/s or lbm/hr

C_c = Specific heat at constant pressure for condenser cooling fluid,
kJ/(kg-°C) or Btu/(lbm-°F)

The evaporator follows the condenser model in the assumption of an overall heat transfer coefficient, U_{EV} , for both the two-phase and superheated regions. According to the author, the following parameters are required by the model:

- Compressor:

V_c = compressor displaced volume, m³ or ft³

r = clearance ratio

n = constant index of polytropic process

w = rotational speed, rad/s

C_v = volumetric coefficient

- Condenser:

T_{ci} = condenser cooling fluid inlet temperature, °C or °F

\dot{m}_c = condenser cooling fluid mass flow rate, kg/s or lbm/hr

C_c = Specific heat at constant pressure for condenser cooling fluid,

J/(kg-°C) or Btu/(lbm-°F)

A_{CD} = heat transfer area of condenser, m² or ft²

U_{CD} = overall heat conductance of condenser, kW/(m²-°C) or Btu/(hr-ft²-°F)

ΔT_{sc} = condenser subcooling, °C or °F

- Expansion valve:

ΔT_s = evaporator superheat, °C or °F

- Evaporator:

T_{hi} = evaporator heating fluid inlet temperature, °C or °F

\dot{m}_h = evaporator heating fluid mass flow rate, kg/s or lbm/hr

C_h = Specific heat at constant pressure for evaporator heating fluid,

kJ/(kg-°C) or Btu/(lbm-°F)

A_{EV} = evaporator heat transfer area, m² or ft²

U_{EV} = overall heat conductance of evaporator, kW/(m²-°C) or Btu/(hr-ft²-°F)

With so many parameters as input data, the author did not provide any information about how to identify these values.

2.1.2.7. Fischer and Rice Model

Fischer and Rice (1983) developed an air-to-air heat pump model to predict the steady-state performance of conventional, vapor compression, electrically-driven heat pumps in both heating and cooling modes. This model is also known as the ORNL Heat

Pump Design Model. The purpose for the development of this model is to provide an analytical design tool for use by heat pump manufacturers, consulting engineers, research institutions, and universities in studies directed toward the improvement of heat pump efficiency.

- *Compressor model*

Since the compressor is the heart of a heat pump system and the primary user of electrical power, accurate compressor modeling is important to good system performance prediction. This criterion, however, must be tempered by consideration of the type of information available to most potential users of the program and of the different types of heat pump studies in which the program may be used. For these reasons the ORNL Heat Pump Design Model does not incorporate a subroutine which rigorously models compressor performance using detailed hardware design parameters. Instead, users can choose between two simpler models depending upon their specific needs: (1) Map-based compressor model, and (2) Loss and efficiency-based compressor model.

The first compressor model is based on the use of compressor manufacturers' data (compressor maps) for a specific compressor or compressor type. The model has built-in corrections to adjust for levels of refrigerant superheat in reciprocating compressor which are different from those for which the maps were generated. Although this model was written for reciprocating compressor, it should be easy to modify for use with rotary,

screw, or centrifugal compressor. Accurate simulation of existing compressor is possible with this model.

The map-based compressor model uses empirical performance curves for reciprocating compressors obtained from compressor calorimeter measurements performed by the manufacturers. These performance curves provide compressor motor power input, refrigerant mass flow rate and/or refrigerating capacity as functions of “evaporator” saturation temperature (i.e., at compressor shell inlet) for four to six “condenser” saturation temperatures (i.e., at the compressor shell outlet). The map-based routine uses curve fits to the compressor motor power input (kW) and the refrigerant mass flow rate (lbm/h) as functions of compressor shell inlet and outlet saturation temperatures to model the published performance data. The user must provide sets of coefficients for bi-quadratic functions of the form given by Equation (2.36) for the power input and mass flow rate as functions of the inlet and outlet saturation temperature.

$$f(T_{outlet}, T_{inlet}) = C_1 T_{outlet}^2 + C_2 T_{outlet} + C_3 T_{inlet}^2 + C_4 T_{inlet} + C_5 T_{outlet} T_{inlet} + C_6 \quad (2.36)$$

where T_{outlet} = inlet saturation temperature, °C or °F

T_{inlet} = outlet saturation temperature, °C or °F

$C_1 - -C_6$ = equation-fit coefficients

The user must also specify the total actual compressor displacement, the rated compressor motor speed, and the fixed refrigerant superheat or temperature at the

compressor shell inlet (upon which the map is based) for the compressor which is being modeled. The desired compressor displacement is also an input parameter. This value is used by the map-based model to scale the compressor performance curves linearly to represent a compressor with the same general performance characteristics as the original compressor but of a different capacity. For values of superheat or suction gas temperature other than those for which the maps were generated, Equations (2.37) and (2.38) are employed for correcting the compressor motor power input and the refrigerant mass flow rate.

$$\dot{m}_{r,actual} = \left[1 + F_V \left(\frac{v_{map}}{v_{actual}} - 1 \right) \right] \dot{m}_{r,map} \quad (2.37)$$

where $\dot{m}_{r,actual}$ = actual refrigerant mass flow rate, kg/s or lbm/hr

F_V = volumetric efficiency correction factor

v_{map} = specific volume under map superheat conditions, m³/kg or ft³/lbm

v_{actual} = specific volume under actual superheat conditions,

m³/kg or ft³/lbm

$\dot{m}_{r,actual}$ = actual refrigerant mass flow rate, kg/s or lbm/hr

$$\dot{W}_{cm,actual} = \left(\frac{\dot{m}_{r,actual}}{\dot{m}_{r,map}} \right) \left(\frac{\Delta h_{isen,actual}}{\Delta h_{isen,map}} \right) \dot{W}_{cm,map} \quad (2.38)$$

where $\dot{W}_{cm,actual}$ = actual compressor motor power input, kW or Btu/hr

$\Delta h_{isen,actual}$ = actual isentropic process enthalpy change, kJ/kg or Btu/lbm

$\Delta h_{isen,map}$ = map isentropic process enthalpy change, kJ/kg or Btu/lbm

$\dot{W}_{cm,map}$ = map compressor motor power input, kW or Btu/hr

The enthalpy gain to the suction gas between compressor shell inlet and suction port due to motor and compressor cooling by the suction gas is assumed as follows.

$$\Delta h_{inlet,suction\ port} = F_{sh} \frac{\dot{W}_{cm,map}}{\dot{m}_{r,map}} \quad (2.39)$$

where F_{sh} = appropriate suction gas heating factor

Once the correction for actual superheat level have been applied to the values of $\dot{W}_{cm,map}$ and $\dot{W}_{r,map}$, the enthalpy at the compressor shell outlet, h_{outlet} , is computed from Equation (2.40).

$$h_{outlet} = (\dot{W}_{cm,actual} - \dot{Q}_{can}) / \dot{m}_{r,actual} + h_{inlet} \quad (2.40)$$

where \dot{Q}_{can} = heat loss rate from the compressor shell, kW or Btu/hr

\dot{Q}_{can} is specified by the user as either a fixed input value or as a specified fraction of actual compressor power.

The second model, a loss and efficiency-based compressor model, is intended for use in heat pump design studies, e.g., to predict how changes in compressor loss and efficiency terms affect system performance. It can also be used to model compressor performance with a new refrigerant. This more general routine models the internal energy balances in a reciprocating compressor using user-supplied heat loss and internal efficiency values. This model cannot predict compressor performance as accurately over the same range of operating conditions as the map-based model without local adjustment of some of the input efficiency and loss values. It is well suited, however, for studying internal compressor improvements and interactions and their effect on system performance about a particular design point.

The loss and efficiency-based compressor routine models the internal energy balance in a reciprocating compressor from user-supplied design, internal efficiency, and heat-loss values. The user is required to specify the following values:

D – total compressor displacement, m³/s or CFM

C – actual clearance volume ratio

S_{input} – synchronous or actual compressor motor speed, RPM

$\dot{W}_{s,fl}$ – compressor motor full load shaft power, kW or Btu/hr

$\eta_{mot,max}$ – maximum compressor motor efficiency

η_{mech} – compressor mechanical efficiency

η_{isen} – isentropic compression efficiency from suction to discharge port

This model can be treated as a supplement to the map-based model since it is not intended to be a rigorous tool to replicate the compressor performance.

- *Expansion device*

The ORNL Heat Pump Design model allows the user to specify a fixed level of condenser subcooling or design parameters for a particular expansion device in order to control the refrigerant flow between the high and low sides of the system. Three basic expansion device models have been developed: capillary tubes, thermostatic expansion valves (TXV), and short-tube orifices.

One of the options in the heat pump model is to simulate the operation of one or more capillary tubes in parallel. The capillary tube model requires the refrigerant pressure and degree of subcooling at the inlet of the capillary tube or tubes. The model consists of empirical fits to curves given in the ASHRAE equipment handbook for a standardized capillary tube flow rate as a function of inlet pressure and subcooling for R-12 or R-22.

The TXV model contains:

- a general model of a cross-charged thermostatic expansion valve
- specific empirical correlations for one size of distributor nozzle and tubes
- additional empirical equations to correct for nonstandard liquid line temperature, tube lengths and nozzle and tube loadings

The short-tube orifice model which is included in the ORNL Heat Pump Design Model uses correlations developed by Mei (1982). He obtained data for five 0.127 m (0.5 in.) long Carrier Accurators with diameters from 1.067 to 1.694 mm (0.0420 to 0.0667 inches) (L/D ratio from 7.5 to 11.9) using R-22. He observed pressure drops between 620 and 1515 kPa (90 and 220 psi) across the restrictor and levels of subcooling from 0 to 28 °C (0 to 50 °F) at the inlet. The observed refrigerant mass flow rates ranged from 68.0 to 213 kg/h (150 to 470 lbm/h).

- *condenser and evaporator model*

The ORNL Heat Pump Design Model calculates the performance of air-to-refrigerant condensers and evaporators by using:

- effectiveness vs. Ntu correlations for heat transfer for a dry coil
- a modified version of the effectiveness surface temperature approach when there is dehumidification
- the Thom correlation for two-phase refrigerant pressure drops and the Moody friction factor chart plus momentum terms for the single-phase refrigerant pressure drops
- friction factor equations for the air-side pressure drop for dry, partially wetted or fully wetted coils.

The calculation method which has been used assumes that the heat exchangers consist of equivalent, parallel refrigerant circuits with unmixed flow on both the air and refrigerant sides. The air-side mass flow rate and the estimated refrigerant mass flow rate

from the compressor model are divided by the number of circuits to obtain values for each circuit. The refrigerant-side calculations are separated into computations for the superheated and two-phase regions for the evaporator and for the superheated, two-phase and subcooled regions for the condenser.

The refrigerant heat transfer coefficient for the superheated region in the condenser is calculated by Equation (2.41) for gas flow from an abrupt contraction entrance.

$$h = C_1 G_r C_{p,v} N_{Pr}^{-2/3} N_{Re}^{C_2} \quad (2.41)$$

where h = heat transfer coefficient, kW/(m²-K), or Btu/(hr-ft²-°F)

C_1, C_2 = constants

G_r = refrigerant mass flux, kg/(m²-s) or lbm/(ft²-hr)

$C_{p,v}$ = refrigerant specific heat, kJ/(kg-K) or Btu/(lbm-°F)

N_{Pr} = Prandtl number

$N_{Re} = G_r D / \mu$, Reynolds number

The refrigerant side or interior heat transfer coefficients for the subcooled region of the condenser and the superheated region in the evaporator are computed using the Dittus-Boelter correlation for fully developed flow.

$$h = 0.023 G_r C_p N_{Pr}^{(C-1)} N_{Re}^{-0.20} \quad (2.42)$$

where h = heat transfer coefficient, kW/(m²-K), or Btu/(hr-ft²-°F)

G_r = refrigerant mass flux, kg/(m²-s) or lbm/(ft²-hr)

C_p = refrigerant specific heat, kJ/(kg-K) or Btu/(lbm-°F)

N_{Pr} = Prandtl number

$N_{Re} = G_r D / \mu$, Reynolds number

C is 0.3 when the refrigerant is being cooled and 0.4 when being heated.

The two-phase heat transfer coefficients for the condenser and the evaporator are average values obtained by effectively integrating local values over the length of the two-phase region. The actual integration is performed over the range of refrigerant quality where a length of tube dz is related to a change in quality of dx by,

$$dz \propto \frac{dx}{h(x)\Delta T} \quad (2.43)$$

and ΔT is the change in temperature between the refrigerant and the tube wall.

The air-side heat transfer coefficients are calculated by Equation (2.44).

$$h_a = C_o G_a C_{pa} N_{Pr}^{-2/3} j \left[\frac{1 - 1280 N_T N_{Re}^{-1.2}}{1 - 5120 N_{Re}^{-1.2}} \right] \quad (2.44)$$

where h_a = heat transfer coefficient, kW/(m²-K), or Btu/(hr-ft²-°F)

G_a = air mass flux, kg/(m²-s) or lbm/(ft²-hr)

$C_{p,a}$ = air specific heat, kJ/(kg-K) or Btu/(lbm-°F)

N_{pr} = Prandtl number

$$j = 0.0014 + 0.2618 \left(\frac{1}{1 - F_a} \right)^{-0.15} \left(\frac{G_a D}{\mu} \right)^{-0.4}$$

N_T = number of tube rows in the heat exchanger in the direction of the air flow

$$N_{Re} = \frac{G_a W_T}{\mu}$$

and $C_o = 1.0, 1.45$ or 1.75 depending on whether the fins are smooth, wavy, or louvered.

The air-side heat transfer coefficient for the portion of the evaporator which is wetted due to dehumidification is calculated from the dry coefficient h_a by Equation (2.45).

$$h_{a,w} = 0.626 \left(\frac{\dot{Q}}{A} \right)^{0.101} h_a \quad (2.45)$$

where $h_{a,w}$ = heat transfer coefficient for wet coil, kW/(m²-°K) or Btu/(ft²-°F)

\dot{Q} = heat transfer rate, kW or Btu/hr

A = frontal area of heat exchanger, m² or ft²

To calculate the performance of the condenser and evaporator, the heat transfer for the liquid, vapor and two-phase refrigerant regions of the heat exchanger are computed using effectiveness vs. Ntu correlations, except for the two-phase refrigerant region of an evaporator with dehumidification. Except for this case, the number of heat transfer units for the two-phase region (condenser and evaporator) is given by Equation (2.46).

$$Ntu = \frac{UA}{C_{\min}} = \left(\frac{A_o}{C_{pm} \left[\frac{A_r}{\eta_a h_a A_a} + \frac{1}{h_{tp}} \right]} \right) \quad (2.46)$$

where Ntu = number of heat transfer units

UA = heat transfer coefficient product, kW/K or Btu/(hr-°F)

C_{\min} = minimum of the heat capacity rates for the air and the refrigerant,
kJ/K or Btu/°F

C_{pm} = specific heat of moist air, kJ/(kg-K) or Btu/(lbm-°F)

A_r = total refrigerant-side heat transfer area, m² or ft²

η_a = heat exchanger overall surface effectiveness

h_a = air side heat transfer coefficient, kW/(m²-K) or Btu/(hr-ft²-°F)

A_a = air side fin and tube heat transfer area, m² or ft²

h_{tp} = average condensing or evaporating heat transfer coefficient,
kW/(m²-K) or Btu/(hr-ft²-°F)

C_{pm} is corrected for moist air conditions (i.e., $C_{pm} = C_{pa} + 0.444 \times W$ where W is the air humidity ratio), A_o is the refrigerant-side heat transfer area per unit of air mass flow rate. The effectiveness is given by Equation (2.47).

$$\varepsilon_{tp} = 1 - e^{-Ntu} \quad (2.47)$$

where ε_{tp} = heat exchanger effectiveness for two phase region

When there is moisture removal on the evaporator, it is assumed to occur only on the two-phase region of the coil.

2.1.2.8. The Comparison by Damasceno, et al.

Damasceno, et al. (1990) compared three steady-state air-to-air heat pump computer models. Two of them are available in the open literature, the third one was developed in-house. These are (1) the MARK III model, which is an updated version of an earlier program developed at Oak Ridge National Lab. by Fischer and Rice (1983) and Fischer et al. (1988) (2) HPSIM, developed at NBS by Domanski and Didion (1983) and (3) HN, developed by Nguyen and Goldschmidt (1986) and updated by Damasceno and Goldschmidt (1987). A summary of predicted capacity and *COP* discrepancies is presented in Table 2.1:

Table 2.1. Interpretation of Accuracy of Performance Predictions

MODEL	HEATING(47 °F)		COOLING(95 °F)	
	CAPACITY	COP	CAPACITY	COP
HPSIM	+15.5%	+7.1%	+3.0%	+7.5%
MARK III	+6.5%	-9.5%	+10.5%	+8.0%
HN	+19.5%	-2.5%	+13.0%	+8.0%

They concluded that the prediction of capacity and coefficient of performance (*COP*) are acceptable for all programs, but they failed to predict detailed refrigerant pressure and temperature distributions adequately.

2.1.2.9. Shelton and Weber Model

Shelton and Weber (1991) developed a chiller model based on manufacturers' performance data. The evaporator was characterized by an overall heat transfer coefficient (UA) function on the cooling load only. The condenser modeling led to a two-parameter correlation of the overall condenser UA with varying water tube velocity and condenser load. The compressor model was based on Carnot efficiency. Assuming an isentropic compressor, constant temperature heat rejection at T_C , and constant temperature heat input at T_E and using the Carnot principle leads to a Carnot-based kW/ton of cooling load calculated as follows:

$$[kW / ton]_{Carnot} = [T_c / T_E - 1] \cdot 3.517 \quad (2.48)$$

where T_C and T_E are in absolute temperature.

This model was corrected by means of compressor isentropic efficiency at design load, which included the motor efficiency, and an efficiency factor that decreased as load decreased due to off-design compressor operation.

$$kW / ton = \frac{[kW / ton]_{Carnot}}{\eta_{ISENT} \eta_{TON}} \quad (2.49)$$

The last two efficiencies (η_{ISENT}, η_{TON}) were determined from second-order polynomial equation equation-fits to the manufacturers' data points.

2.1.2.10. Greyvenstein Model

A computer model for the simulation of vapor-compression heat pumps and refrigeration systems with thermo-statically controlled expansion valve is presented. The model describes the performance of the system given its design, the fan curves, the compressor characteristics, the design of the heat exchangers and the condition of the external fluids flowing through the heat exchangers.

The compressor model consists of a performance data file and an interpolation routine which uses the data in the file to interpolate values of refrigerant mass flow and input power given the inlet and outlet pressures. The accuracy of the model therefore depends on the accuracy of the performance data. The evaporator is of fin and tube type in a stream of air. The heat absorbed by the refrigerant in the evaporator can be divided into two parts. The first part is the heat necessary to evaporate all the liquid, while the second part is that necessary to heat the vapor to the superheated point. The heat absorbed by the refrigerant is transferred across the outside surface area of the evaporator. The total outside surface area can thus also be divided into two parts associated with the quantities of those two parts of the heat. The two air streams across the two parts are mixed after the evaporator. From the heat transfer relationships, we may have:

$$Q = UA\Delta T \quad (2.50)$$

where U = overall heat transfer coefficient, kW/(m²-K) or Btu/(hr-ft²-°F)

ΔT = log mean temperature difference, °C or °F

$$A = \text{area, m}^2 \text{ or ft}^2$$

For two-phase region and superheated region, different correlations and equations are used for the U , ΔT and A respectively.

Similarly, the heat rejected by the refrigerant can be divided into three parts in the condenser. The first part is the heat necessary to cool the superheated refrigerant to saturated vapor. The second part is the heat associated with the condensation of the saturated vapor. The third part is the heat rejected in sub-cooling the saturated liquid. The heat transfer relationships are established from the same principle as evaporator.

The evaporator model was verified by comparing it with design data published by the Bohn Heat Transfer Division of the Gulf and Western Metals Forming Company. The Bohn data are based on laboratory findings and widely used in the refrigeration industry for the design of evaporator coils. No experimental data are available for the type of condenser. Some related data are adapted to this type, which is essentially the same as the water-cooled kind.

The author claimed that the model is a powerful and versatile tool for the design and optimization of refrigeration systems or heat pumps and has been used successfully to design a number of systems.

2.1.2.11. Dabiri Model

A steady state heat pump simulation model was developed by Dabiri (1982) that targeted at reducing the amount of testing required by DOE to obtain heat pump performance rating information. The Fisher and Rice (1981) air-to-air heat pump model that developed for design purposes was modified. Power inputs to indoor and outdoor fans, which were calculated as outputs in the original model, were inputs to this simulation model. Other modification such as a reversing valve model and refrigerant line losses was also discussed. The input variables to the heat pump simulation model for each component include redundant information that normally available for a research lab. For example, the required inputs for the condenser and evaporator are: outside diameter of tubes, inside diameter of tubes, fin thickness, fin pitch and configuration, thermal conductivity of the fins, heat exchanger frontal area, number of tubes in direction of airflow, number of parallel circuits in heat exchanger, spacing of tube passes perpendicular to airflow, spacing of tube rows in direction of airflow, total number of return bends in heat exchanger, and contact conductance between fins and tubes. The model's outputs include heating capacity, *COP*, mass flow rate through the compressor, refrigerant pressure and temperature at every point of the circuit, air pressure drops across the heat exchanger, and air temperature at the heat exchangers' exits. Compressor shell heat loss was considered in the model and no specific pattern exists in the relationship between the shell heat loss and evaporating temperature was observed. The compressor shell heat loss factor varied between 10% and 40%. The heat pump simulation model was applied to three different heat pumps and results were presented. The results presented

indicate that the simulation model predictions generally fall within the acceptable tolerance of the ARI standards and within the possible errors existing in the experimental measurements. A sensitivity analysis was made to assess the effect of possible variation of some of the inputs parameters on the system's thermal performance. The input parameters that could not be determined accurately were listed.

2.1.2.12. Ouazia and Snelson's Model

Ouazia and Snelson (1994) presented a simulation model suitable for the preliminary evaluation of refrigerants and refrigerant mixtures in a water-water heat pump test facility. The simulation is specific to the heat pump test facility and uses a semi-theoretical cycle analysis to predict steady-state operating conditions. The model is to calculate performance characteristics including evaporator capacity, compressor shaft power, refrigerant mass flow, cooling coefficient of performance, etc.

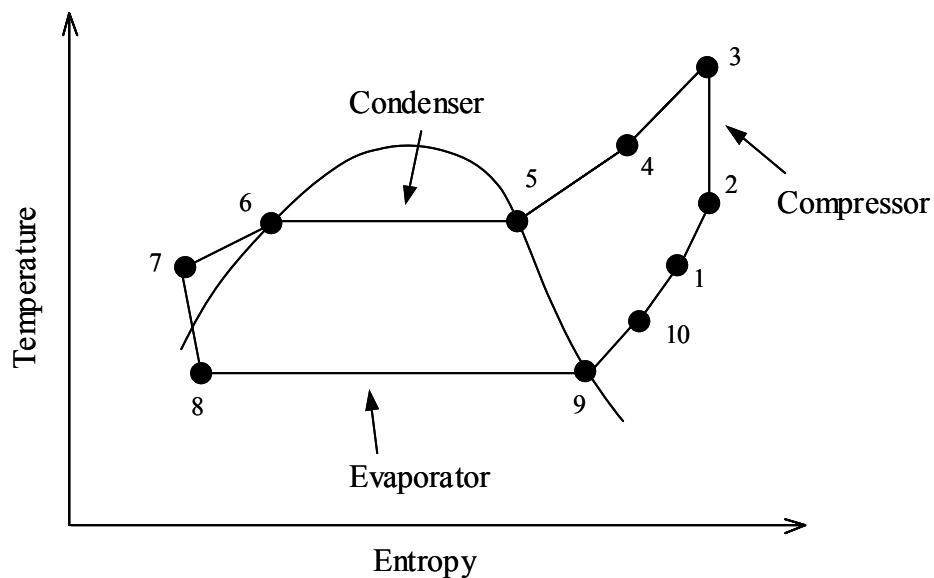


Figure 2.6. Temperature-entropy diagram for the simulated heat pump

The simulation uses a simplified model of an open-drive reciprocating compressor, and includes effects such as refrigerant subcooling at the condenser outlet, refrigerant superheating at the evaporator outlet, heat transfer and pressure drops in heat exchangers, and a representation of liquid line/suction line heat exchange. The temperature-entropy diagram shown in Figure 2.6 represents the basic vapor-compression cycle as modeled by the computer simulation. Assumptions made are: compression process 2-3 is isentropic; expansion process 7-8 is isenthalpic; condensation and evaporation processes are at constant pressure. To use the simulation program, it is necessary to specify the evaporator superheat, condenser exit subcooling, and secondary side temperatures for the condenser and evaporator. Initial estimates must also be provided of the refrigerant saturation temperatures at the condenser and evaporator and for the refrigerant mass flow rate.

2.1.2.13. Krakow and Lin's Model

A computer model of a multiple-source heat pump was presented by Krakow and Lin (1983). The model was used to simulate heat pump systems having solar insolation, ambient air, or storage water as energy source and space air or storage water as energy sink. The model determines steady-state performance characteristics of a heat pump interacting with the environment. The evaporators and condensers in the system are specified by values of heat exchanger effectiveness and heat capacities. The values of heat capacities of evaporators and condensers depend on the flow rate of air or water, not those of the refrigerant. For constant air or water flow rates, the values of heat capacities and heat exchanger effectiveness are assumed constant.

The compressor model permits the simulation of heat pump systems with reciprocating compressors. The performance of a reciprocating compressor is specified by,

$$e_{vi} = 1 + c - c \cdot (P_c / P_e)^{1/n} \quad (2.51)$$

$$e_v = e_r \cdot e_{vi} \quad (2.52)$$

$$m = e_v \cdot V / v \quad (2.53)$$

$$e_i = (h_{coi} - h_{ci}) / (h_{coa} - h_{ci}) \quad (2.54)$$

where c = clearance volume ratio

e_i = isentropic compression efficiency

e_r = volumetric efficiency ratio, actual/theoretical

e_v = actual volumetric efficiency of the compressor

e_{vi} = ideal volumetric efficiency of the compressor

h_{ci} = enthalpy at compressor inlet, kJ/kg or Btu/lbm

h_{coa} = actual enthalpy at compressor outlet, kJ/kg or Btu/lbm

h_{coi} = ideal enthalpy at compressor outlet, kJ/kg or Btu/lbm

m = refrigerant mass flow rate, kg/s or lbm/m

n = ratio of specific heats of the refrigerant vapor

P_c = condensation pressure, kPa or psi

P_e = evaporation pressure, kPa or psi

v = refrigerant specific volume at compressor inlet, m³/kg or ft³/lbm

V = rate of volumetric displacement, m³/s or CFM

An air-cooled or a water-cooled condenser was simulated. The following equations were used to specify the performance of the condenser,

$$Q_c = e \cdot H \cdot (T_c - T_{snk}) \quad (2.55)$$

$$e = (T_{hot} - T_{snk}) / (T_c - T_{snk}) \quad (2.56)$$

where e = heat exchanger effectiveness

H = heat capacity of space air or storage water, energy/time/degree temperature difference, kW/°C or Btu/(hr-°F)

Q_c = condenser heat transfer rate, energy/time, kW or Btu/hr

T_c = condensation temperature of the refrigerant, °C or °F

T_{snk} = inlet temperature of space air or storage water, °C or °F

T_{hot} = outlet temperature of space air or storage water, °C or °F

The heat pump under investigation used solar/air collectors, through which ambient air was circulated during the night and periods of low solar insolation. The collector's performance as an evaporator extraction heat from ambient air is specified by the heat capacity of the source and the heat exchanger effectiveness. A water-cooled storage evaporator may also be the same parameter. The performance of either of these evaporators is governed by,

$$Q = e \cdot H \cdot (T_{src} - T_e) \quad (2.57)$$

where e = heat exchanger effectiveness

H = heat capacity of the source, energy/time/degree temperature

difference, kW/°C or Btu/(hr-°F)

Q = rate of energy absorbed by refrigerant, energy/time, kW or Btu/hr

T_e = evaporation temperature, °C or °F

T_{src} = source temperature, ambient air or storage water, °C or °F

2.2. Modeling of Heat Pump Components

Models for heat transfer process and primary components (i.e. heat exchangers, compressor, expansion devices) of heat pumps or chillers are focus of this section. Only models relevant to the basic heat pump components and fundamental techniques that might be useful in the future research work are discussed.

2.2.1. Analysis of Heat Transfer between Moist Air and Cold Surface by McElgin and Wiley

The transfer of heat from warm moist air to cold surface and thence through the fins and tubes to the cold water or refrigerant may best be analyzed by dividing the process into two distinct steps, (1) from the air to the wetted surface and (2) from the surface through the fins and tubes to the water. The total heat lost by the air in passing over an element of wetted area dA_w is given by:

$$dH_T = \frac{f_g}{s} (h - h_s) dA_w \quad (2.58)$$

where H_T = total heat lost by total weight of air flowing over wetted surface,

kW or Btu/hr

f_g = sensible heat transfer coefficient, kW/(m²-K) or Btu/(hr-ft²-°F)

s = humid specific heat of air vapor mixture, kJ/(kg-K) or Btu/(lbm-°F)

h = total heat content of air vapor mixture per mass of dry air,

kJ/kg or Btu/lbm

h_s = total heat content of air vapor mixture per mass of dry air at surface,
kJ/kg or Btu/lbm

This equation which was originally derived by Merkel (1925), combines sensible heat transfer due to temperature difference and latent heat transfer due to vapor pressure difference into a single equation which states that the rate of simultaneous sensible and latent heat flow depends on the difference between the total heat of the air flowing over the surface and the total heat corresponding to saturation at the surface temperature. The total heat transferred from the element of area dAw through the fins and tubes to the water is given by:

$$dH_T = \frac{1}{R}(t_s - t_R)dAw \quad (2.59)$$

where t_s = surface temperature, °C or °F

t_R = refrigerant temperature, °C or °F

Where R is as defined above the composite resistance to heat flow imposed by the fins and tubes and the internal water film. Equations (2.58) and (2.59) are rearranged:

$$\frac{t_s - t_R}{h - h_s} = \frac{f_g R}{s} = C \quad (2.60)$$

The value of s , the humid specific heat of air, may be taken as constant for the range of comfort cooling. For a given coil, air velocity and refrigerant velocity, f_g and R are constant and thus C is a constant coil characteristic for given conditions.

2.2.2. Analysis of Air Side Heat Transfer in Finned Tube Heat Exchangers by Webb

When heat is transferred between air and sensible or two-phase fluids in tubes, finned tube heat exchangers are beneficial. In this case, the air-side heat transfer coefficient may be 10-50 times smaller than the tube-side coefficient. The use of a finned surface will increase the air-side conductance (hA) to more evenly proportion the thermal resistance on each side of the heat exchanger. In many applications, air-side extended surface can be added for much less unit cost than that if the base tube surface. The degree of heat transfer augmentation is dependent on the following factors:

- 1) Fin spacing
- 2) Fin efficiency
- 3) Use of special fin configuration to yield increased heat transfer coefficients

The significance of these factors on the resulting augmentation is given by Equation (2.61), which defines the overall heat transfer coefficient, based on the internal tube area:

$$\frac{1}{U} = \frac{A_i}{\eta h A} + \frac{1}{h_i} \quad (2.61)$$

where U = overall heat transfer coefficient, kW/(m²-°K) or Btu/(hr-ft²-°F)

A_i = inside surface area, m² or ft²

η = total surface efficiency

Thus, the air-side conductance is:

$$K = \frac{\eta h A}{A_i} \quad (2.62)$$

An increased number of fins per centimeter will increase the conductance by increase the conductance by increase the ratio A/A_i . Also, the use of more closely spaced flat fin will increase the heat transfer coefficient h , because of a smaller hydraulic diameter. Or, the use of a special fin configuration, such as a “wavy” fin, will produce a higher heat transfer coefficient. The surface efficiency η is influenced by the fin thickness, thermal conductivity, and fin length. The fin efficiency may be calculated from appropriate graphs or equations given in most heat transfer textbook. The surface efficiency is calculated from Equation (2.63):

$$\eta = 1 - \frac{A_f}{A} (1 - \eta_f) \quad (2.63)$$

where A is the total external surface and A_f is the finned surface area.

2.2.3. Experimental Results of Chilled-Water Cooling Coils Operating at Low Water Velocities by Mirth et al.

Experimental results were presented that demonstrate that chilled-water cooling coils operating at low water-side Reynolds numbers do not perform as well as predicted by the manufacturer’s software. The manufacturer’s software overpredicts coil performance by as much as 8% at a water-side Reynolds number of 3100 (the lower Reynolds number limit certifiable under ARI standard 410-87). At a Reynolds number of

2300, the overpredictions range from 12% to 18%. An analysis revealed that this problem could be mitigated by using the Gnielinski correlation instead of the Dittus-Boelter correlation to predict the water-side heat transfer coefficient. When the coils were operating in the turbulent flow regime ($Re_w > 2300$), a coil model using the Gnielinski correlation was able to predict coil performance to within 4% for wet fin surface conditions and to within 2% for dry surface conditions. A laminar, developing flow correlation that was tested for water-side Reynolds numbers less than 2300 underpredicted coil performance.

2.2.4. Comparison of Methods of Modeling the Air Side Heat and Mass Transfer in Chilled-Water Cooling Coils by Mirth and Ramadhyani

Three different methods of modeling the heat and mass transfer in chilled-water cooling coils are compared. A new model (model 3) is compared with discretized version of the models presented in ARI Standard 410-87 (model 1) and by McQuiston (model 2) and with the ARI log-mean enthalpy method. The models differ both in the method used to determine the heat transfer rate to primary surface and in the method used to determine the fin efficiency. It was summarized that the heat transfer rate predicted by model 1 agreed within 1% to 2% of the new model, while model 2 predicted heat-transfer rates 2% to 8% higher than did model 3. However, by modifying the assumptions used in model 2, it was possible to bring its predictions to within 2% of those of model 3. The ARI log-mean enthalpy method was also found to agree well within 2%.

2.2.5. Cooling Coil Model of Braun, et al.

Braun, et al. (1989) proposed an effectiveness model for cooling coils. The cooling coil model was developed from a basic analysis of cooling tower performance. The primary difference between the analysis of cooling coils and cooling towers is associated with the fact that the air and water streams are not in direct contact. A schematic of a counter-flow cooling tower showing the important states and dimensions is given in Figure 2.7.

From steady state energy and mass balances on an incremental volume, the following differential equations may be derived:

$$\frac{d\omega_a}{dV} = -\frac{Ntu}{V_T}(\omega_a - \omega_{s,w}) \quad (2.64)$$

$$\frac{dh_a}{dV} = -\frac{LeNTU}{V_T} \left[(h_a - h_{s,w}) + (\omega_a - \omega_{s,w})(1/Le - 1)h_{g,w} \right] \quad (2.65)$$

$$\frac{dT_w}{dV} = \frac{\frac{dh_a}{dV} - C_{p,w}(T_w - T_{ref})\frac{d\omega_a}{dV}}{\left[\frac{\dot{m}_{w,i}}{\dot{m}_a} - (\omega_{a,o} - \omega_a) \right] C_{p,w}} \quad (2.66)$$

where $Le = \frac{h_c}{h_D C_{p,a}}$

$$Ntu = \frac{h_D A_V V_T}{\dot{m}_a}$$

A = surface area, m² or ft²

A_v = surface area of water droplets per volume of cooling tower, m^2 or ft^2

$C_{p,a}$ = constant pressure specific heat of moist air, $kJ/(kg-K)$ or

$Btu/(lbm-^{\circ}F)$

$C_{p,w}$ = constant pressure specific heat of liquid water, $kJ/(kg-K)$ or

$Btu/(lbm-^{\circ}F)$

C_s = derivative of saturation air enthalpy with respect to temperature,

$kJ/(kg-K)$ or $Btu/(lbm-^{\circ}F)$

C^* = ratio of air to water capacitance rate for dry analysis

h_a = enthalpy of moist air per mass of dry air, kJ/kg or Btu/lbm

h_c = convection heat transfer coefficient, $kW/(m^2-K)$ or $Btu/(hr-ft^2-^{\circ}F)$

h_D = mass transfer coefficient, $kg/(m^2-s)$ or $lbm/(ft^2-hr)$

h_g = enthalpy of water above reference state for liquid water at T_{ref} , kJ/kg

or Btu/lbm

h_s = enthalpy of saturated air, kJ/kg or Btu/lbm

\dot{m}_w = mass flow rate of water, kg/s or lbm/hr

\dot{m}_a = mass flow rate of dry air, kg/s or lbm/hr

m^* = ratio of air to water effective capacitance rate for wet analysis

Le = Lewis number

Ntu = overall number of transfer units

\dot{Q} = overall heat transfer rate, kW or Btu/hr

T_a = air temperature, $^{\circ}C$ or $^{\circ}F$

T_{ref} = reference temperature for zero enthalpy of liquid water, °C or °F

T_s = surface temperature, °C or °F

T_w = water temperature, °C or °F

UA = overall heat transfer conductance, kW/K or Btu/(hr-°F)

V = volume, m³ or ft³

ϵ_a = air side heat transfer effectiveness

ω_a = air humidity ratio, kg/kg dry air

ω_s = humidity of saturated air, kg/kg dry air

Subscripts:

a = air stream conditions

dry = dry surface

e = effective

i = inlet or inside condition

o = outlet or outside conditions

s = surface conditions

T = total

w = water stream conditions

wet = wet surface

In order to simplify the analysis, Merkel made two assumptions:

- The water loss due to evaporation is neglected, such that the water flow rate at each point in the tower is constant and equal to the inlet flow.

- A Lewis number of unity is also assumed.

With these approximations, the equation for the cooling tower may be reduced to:

$$\frac{dh_a}{dV} = -\frac{Ntu}{V_T}(h_a - h_{s,w}) \quad (2.67)$$

$$\frac{dT_w}{dV} = \frac{\dot{m}_a (dh_a / dV)}{\dot{m}_w C_{p,w}} \quad (2.68)$$

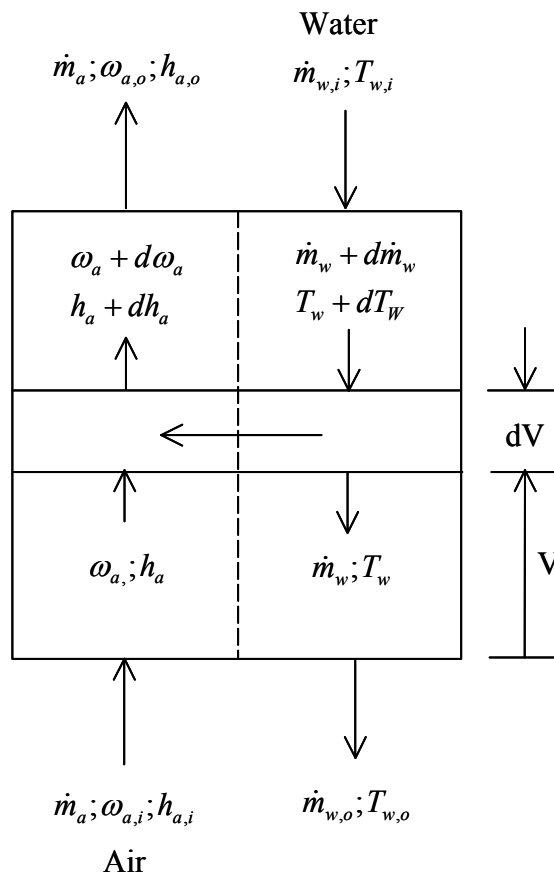


Figure 2.7. Schematic of a counter-flow cooling tower

Equation (2.68) may be rewritten in term of air enthalpies only by introducing the derivative of the saturated air enthalpy with respect to temperature evaluation at the water temperature.

$$\frac{dh_{s,w}}{dV} = \frac{\dot{m}_a C_s (dh_a / dV)}{\dot{m}_w C_{p,w}} \quad (2.69)$$

$$\text{where } C_s = \left[\frac{dh_s}{dT} \right]_{T=T_w}$$

C_s has the units of specific heat and will be termed the saturation specific heat. According to the authors, through the introduction of the air saturation specific heat and thus the effectiveness relationships, this approach has several advantages such as simplicity, accuracy and consistency with the methods for analyzing sensible heat exchangers. This paper presented the basic equations for effectiveness relationships for cooling coils analogous to those for sensible heat exchangers, and also provided a procedure to estimate the performance of a cooling coil having both wet and dry portions. The method was validated over wide range of conditions. The steps for determining the heat transfer and outlet conditions for a cooling coil are summarized as follows,

- 1) Assume that the coil is completely dry and apply the dry coil effectiveness method.
- 2) If the surface temperature at the air outlet determined with the dry analysis is less than the dew point of the entering air, then assume that the coil is completely wet and apply the wet coil effectiveness method.

- 3) If the surface temperature at the air inlet determined with the wet analysis is greater than the entering dew point temperature, then a portion of the coil is dry. At this point, the fractions of the coil that are wet and dry could be determined iteratively. More simply, choose the result of steps 1 or 2 that yields the largest heat transfer.

In order to simulate the performance of a cooling coil in a system, it is necessary to estimate the air side and water side transfer units as a function of the flows. In other words, the heat transfer coefficients UA 's are essential if the mass flow rate and specific heat are given according to the definition of NTU. Without specific details concerning the dimensions and configuration of the coil, the NTU is not readily available. The author provides an empirical solution as,

$$Ntu_i = k_1 \left[\frac{\dot{m}_w}{\dot{m}_{w.des}} \right]^{k_2} \quad (2.70)$$

$$Ntu_o = k_3 \left[\frac{\dot{m}_a}{\dot{m}_{a.des}} \right]^{k_4} \quad (2.71)$$

where \dot{m}_w = water mass flow rate, kg/s or lbm/hr

\dot{m}_a = mass flow rate of dry air, kg/s or lbm/hr

The author did not provide any information about how to get the values of so-called $\dot{m}_{w.des}$ and $\dot{m}_{a.des}$. But according to the form of Equations (2.70) and (2.71) which employs one of the commonly used regression techniques, they should have the values of some base case, say nominal flow rates for the heat exchanger. k_1 , k_2 , k_3 and k_4 are empirical

constants that may be determined with nonlinear regression applied to differences between measurements and cooling coil model predictions of the water and air outlet temperatures. This approach may not be feasible for modeling the chiller or heat pump because the detailed catalog data for the heat exchanger are usually not available from the chiller or heat pump manufacturers' catalog.

2.2.6. Parameter Estimation Technique of Rabehl, et al.

Rabehl, et al. (1999) presented a technique for developing models that can accurately reproduce cooling coil performance. This technique employed mechanistic relations with unspecified parameters as the basis for model relations. Catalog information is then used to estimate the optimal values of the parameters. Only a few geometric specifications are required. This technique is based on the fundamental heat and mass transfer correlations that are manipulated so that all geometric terms are lumped into characteristic parameters. Then the values of parameters are determined from curve fits to catalog data.

The author classified the models for heat exchangers by the degree of complexity and empiricism incorporated. Two extreme ends exist: at one end of the spectrum are simple models that highly empirical and require few geometry specifications; at the other end, detailed models for heat exchangers and coils have been developed. These detailed models are based on fundamental heat and mass transfer relations, but many require details on construction that are not often available from manufacturers' catalogs.

For chilled water cooling coil, the overall heat and mass transfer coefficient was assumed to be based on two heat transfer resistances in series: the convection heat transfer resistance between the tube fluid (e.g. chilled water) and the tube wall; and the convection heat transfer resistance between the tube/fin surface and the air. The resistance of the heat exchanger wall is neglected. The two convection resistances are assumed to have the same form of heat transfer coefficient:

$$Nu_D = C Re_D^m Pr^n \quad (2.72)$$

where C , m , and n are specific values for a given flow geometry. For the heat transfer coefficient between the tube/fin surface and the air, the Nusselt number relation of Zhukauskas was used as the basis for the model. Equation (2.72) was modified by introducing parameters that account for specific characteristics such as flow area, surface area, tube bank arrangement, fin efficiency, and fluid type. Generalizing Equation (2.72) yielded an equation for the heat transfer coefficient-area product in terms of the mass flow rate and fluid properties:

$$(hA)_o = C_f C_1 k_o \left(\frac{\dot{m}_o}{\mu_o} \right)^{C_2} Pr_o^{0.36} \left(\frac{Pr_o}{Pr_{o,s}} \right)^{0.25} \quad (2.73)$$

where C_1 and C_2 are parameters that need to be determined. The effect of property variations across the flow were expressed as a Prandtl number ratio since the external

fluid is air. C_f is a convection coefficient correction factor that accounts for the totally wet operation.

The heat transfer coefficient between the inner fluid and the tube wall was based on the Sieder-Tate equation. In a manner similar to that for Equation (2.73), the relation for the heat transfer coefficient-area product inside the tubes was modified to be:

$$(hA)_i = C_3 k_i \left(\frac{\dot{m}_i}{\mu_i} \right)^{0.8} \text{Pr}_i^{1/3} \left(\frac{\mu_i}{\mu_{i,s}} \right)^{0.14} \quad (2.74)$$

The values of the three characteristic heat transfer parameters C_1 , C_2 and C_3 need to be fit using catalog data points.

2.2.7. Reciprocating Compressor Model of Popovic and Shapiro

Popovic and Shapiro (1995) proposed a semi-empirical model for modeling a reciprocating compressor in refrigeration systems simulations. The model is based on thermodynamics principles and a large database. The purpose of the model is to reduce the amount of data required to completely characterize compressor performance using alternative refrigerants. Two compressor performance parameters were defined. An effective pressure drop accounts for mass flow losses in the compressor, while numerically determined functional dependence of the heat transfer loss coefficient is related to compressor energy losses. The model depicted compressor operation with

reasonable accuracy. The model predicted mass flow rates and required compressor power for all data points within 10% of relative error.

As claimed by the authors, the McQuiston and Parker (1994) volumetric efficiency compressor model was the starting point in the model development. Several assumptions are incorporated into the modeling procedure. The final equation determining the refrigerant mass flow rate through the compressor is:

$$\dot{m} = \frac{RPD \cdot RPM}{v_{suc}} \left[1 + C - C \left(\frac{P_{dis}}{P_{suc}} \right)^{1/n} \right] \quad (2.75)$$

where \dot{m} = refrigerant mass flow rate, kg/s or lbm/hr

RPD = rate of piston displacement, m³/RPM or ft³/RPM

RPM = compressor motor shaft speed (revolutions per minute)

v_{suc} = specific volume for suction state, m³/kg or ft³/lbm

C = clearance factor

P_{dis} = pressure at discharge state, kPa or psia

P_{suc} = pressure at suction state, kPa or psia

n = polytropic exponent

However, according to the literature survey, Threlkeld might be the first researcher who systematically presented the thermodynamic description of a mechanical vapor compression refrigeration cycle. In the book titled ‘Thermal Environmental Engineering’ published in 1962, he provided a few important definitions and equations that are still

widely used nowadays. The coefficient of performance expresses the effectiveness of a refrigeration system, it is a dimensionless ratio defined by the expression:

$$C.O.P. = \frac{\text{Useful Refrigerating Effect}}{\text{Net Energy Supplied From External Source}} \quad (2.76)$$

For a mechanical-compression system, work must be supplied by an external source, thus:

$$C.O.P = \frac{Q}{W} \quad (2.77)$$

where Q = refrigeration capacity, kW or Btu/hr

W = power consumption, kW or Btu/hr

In the model developed by Popovic and Shapiro (1995), the comparison was originally run assuming no pressure drops. Refrigerant mass flow rates calculated by Equation (2.75) significantly overestimated the measured mass flow rate. Thus, the presence of suction and discharge pressure drops was considered. Pressure drops were assumed to be processes with constant enthalpy in order to fix suction and discharge states for the compressor. To simplify the problem, the magnitudes of the suction and discharge pressure drops were set equal.

Accurate prediction of a refrigerant mass flow rate requires knowledge of the clearance factor, pressure drops, polytropic exponent, refrigerant inlet state, and

refrigerant outlet pressure. The clearance factor is a compressor design parameter that depends on compressor cylinder geometry. Unfortunately, compressor manufacturers were not willing to release this information. Hence, the clearance factor had to be taken as unknown parameter. The pressure drops were also taken as unknown, but were set equal to each other. In order to determine these three compressor parameters it was decided to vary each one looking for the minimum relative error between the calculated and measured mass flow rates.

2.2.8. ARI Standard 540-99

ARI standard 540-99 is to establish for positive displacement refrigerant compressors and compressor units for refrigeration application. This standard is intended for the guidance of the industry, including manufacturers, engineers, installers, contractors and users. In this standard, it is required that general performance data, covering the operational spectrum of the equipment be presented in tabular form within defined accuracies and ranges of operation. It is also required that a third order polynomial equation of 10 coefficients be used to represent the tabular data in the following form,

$$\begin{aligned}
 X = C_1 + C_2 \times (S) + C_3 \times D + C_4 \times (S^2) + C_5 \times (S \times D) + C_6 \times (D^2) + C_7 \times (S^3) \\
 + C_8 \times (D \times S^2) + C_9 \times (S \times D^2) + C_{10} \times (D^3)
 \end{aligned}
 \tag{2.78}$$

Where C = equation coefficient, represents compressor performance

S = suction dew point temperature, °C or °F

D = discharge dew point temperature, °C or °F

X represents (as designated):

Power input, W or kW

Mass flow rate, lbs/hr or kg/hr

Current, A

Compressor or compressor unit efficiency

2.2.9. Ganesh et al. Coil Model

A new coil model (Ganesh 1987) for cooling and heating was employed by Ganesh et al. (1989) as a component in the overall system with either single phase (chilled or hot water coil) or two phase (DX or steam coil) fluid through the tubes. The effect of various coil parameters on the overall HVAC system performance was also studied.

Ganesh (1987) modeled steady state performance of heating and cooling coil with both one and two phase heating or chilled fluid flowing through the tubes. Once the inlet conditions of air and tube fluid is specified along with coil geometric configuration, the outlet conditions are predicted. The inlet air conditions include air flow rate, maximum air velocity, dry and wet bulb air temperatures. Coil configuration to be specified includes coil face area (length and height), tube outside diameter and thickness, tube, row and fin spacings and number of rows. If single phase fluid is used through tubes, inlet conditions are fluid velocity and temperature while for two phase fluid the inlet conditions is just the evaporating or condensing temperature.

In single phase flows, fluid inlet temperature and velocity are specified. In typical performance type calculation the length and height of the coil are specified and the temperature drop or rise is obtained from the program. In addition the program also calculates outlet air dry and wet bulb temperatures along with the total heat transfer. Coil circuitry is important since it influences the liquid mass flow and a standard coil with single row serpentine configuration and 'U' bends at opposite ends was assumed. In two phase flows, the inlet and exit conditions are fixed for the tube fluid and the mass flow rate is iterated such that both the thermodynamic and heat transfer relations are satisfied by suitable adjustments to the aspect ratio, if necessary. The output from the program is outlet air dry and wet bulb conditions and the total heat transfer. Sensible and latent components are also calculated. Coil circuitry is not critical for heat transfer calculation since the mass flow rate is iterated for convergence.

The following assumptions were made:

- 1) Heat transfer between heat exchanger and surroundings is negligible and that there are no thermal energy sources within the heat exchanger.
- 2) Only transverse heat flow across the tube wall is considered. First law of thermodynamics (ignored kinetic and potential energy changes) for an open system applied to both air side and tube fluid side. The heat exchanger equation (cross or counter-flow) is described by the log-mean temperature difference for the dry coil and by the log-mean enthalpy difference for the wet coil.

- 3) Thermophysical properties of moist air and tube fluid due to total pressure drop through the heat exchanger is negligible.

The main criteria used to determine whether a cooling coil is completely dry or completely wet or partially dry/wet is analogous to that used by Elmahdy and Mitalas:

- 1) If coil surface temperature at air inlet section is less than the dew point temperature of air at the inlet then the coil surface is all wet.
- 2) If the surface temperature at the air outlet section is greater than the dew point temperature of air at the inlet then the coil is completely dry.
- 3) If neither 1 or 2 is satisfied then the coil is partially dry/wet.

The derivation of the equations for the dry and wet portions of the coil is given in detail by Elmahdy and Mitalas (1977).

- *Cooling coil model for single phase tube fluid*

For cooling coils it is possible that dehumidification starts occurring at some point along the length of the coil when the coil surface temperature is less than the dew point temperature. This identification of the boundary is important since different equations and correlations apply to the dry and wet portion of the coil. Figure 2.8 gives a schematic of a cooling and dehumidifying coil along with the appropriate variables.

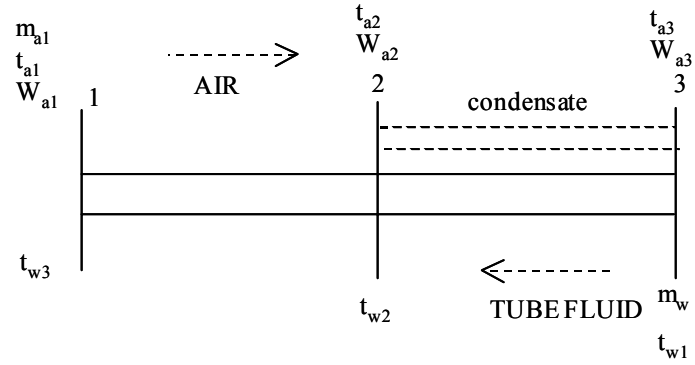


Figure 2.8. Schematic of cooling and dehumidifying coil

Dry surface:

$$Q = (t_{a1} - t_{a2}) / X \quad (2.79)$$

$$Q = (t_{w2} - t_{w3}) / Y \quad (2.80)$$

$$Q = U_{od} A_{od} \Delta t_{lm} \quad (2.81)$$

where $X = 1 / (m_a C_{pa})$

$$X = -1 / (m_w C_{pw})$$

$$\Delta t_{lm} = \frac{(t_{a1} - t_{w3}) - (t_{a2} - t_{w2})}{\ln(t_{a1} - t_{w3}) / (t_{a2} - t_{w2})}$$

Q = heat transfer rate, kW or Btu/hr

t_{a1} = entering air temperature, °C or °F

t_{a2} = air temperature at interface, °C or °F

t_{w2} = tube fluid temperature at interface, °C or °F

t_{w3} = leaving tube fluid temperature, °C or °F

U_{od} = overall heat transfer coefficient, dry, kW/(m²-°C) or Btu/(hr-ft²-°F)

A_{od} = tube outside area, m² or ft²

Δt_{lm} = log mean temperature difference, °C or °F

m_a = air mass flow rate, kg/s or lbm/hr

C_{pa} = air specific heat, kJ/(kg-°C) or Btu/(lbm-°F)

m_w = tube fluid mass flow rate, kg/s or lbm/hr

C_{pw} = tube fluid specific heat, kJ/(kg-°C) or Btu/(lbm-°F)

Solving the above system,

$$t_{a2} = t_{a1} - K_1(t_{a1} - t_{w2}) \quad (2.82)$$

$$t_{w3} = t_{a1} - K_2(t_{a1} - t_{w2}) \quad (2.83)$$

where $K_1 = X(Z - 1)$

$$K_2 = Z(X + Y) / W$$

$$Z = \exp\{U_{od} A_{od} (X + Y)\}$$

$$W = XZ + Y$$

Coil surface temperature is computed from

$$(t_{s2} - t_{w2}) / (t_{a2} - t_{w2}) = (\sum R - R_o) / \sum R \quad (2.84)$$

where $\sum R = R_i + R_f + R_p + R_c + R_o = 1 / (U_{od} A_{od})$

$$R_i = 1 / (h_i A_{pid})$$

$$R_f = F / A_{pid}$$

$$R_p = \delta_t / (k_t A_{pid})$$

$$R_c = 1 / (A_{po} h_c)$$

$$R_o = 1 / (h_{od} \eta_{od} A_{od})$$

t_{s2} = coil surface temperature, °C or °F

R_o = outside tube thermal resistance, m²-°C/kW or hr-ft²-°F/Btu

R_i = inside tube thermal resistance, m²-°C/kW or hr-ft²-°F/Btu

R_f = fin thermal resistance, m²-°C/kW or hr-ft²-°F/Btu

R_p = tube thermal resistance, m²-°C/kW or hr-ft²-°F/Btu

R_c = calculated thermal resistance, m²-°C/kW or hr-ft²-°F/Btu

h_i = inside tube film heat transfer coefficient, kW/(m²-°C) or
Btu/(hr-ft²-°F)

A_{pid} = area, m² or ft²

F = fouling factor

δ_t = tube thickness, m or ft

k_t = tube conductivity, kW/(m-°C) or Btu/(hr-ft-°F)

A_{po} = area, m² or ft²

h_c = calculated film heat transfer coefficient, kW/(m²-°C) or
Btu/(hr-ft²-°F)

h_{od} = outside tube heat transfer coefficient, kW/(m²-°C) or Btu/(hr-ft²-°F)

η_{od} = fin effectiveness

wet surface:

$$Q = (h_{a2} - h_{a3}) / X' \quad (2.85)$$

$$Q = (h_{sw1} - h_{sw2}) / Y' \quad (2.86)$$

$$Q = U_{ow} A_{ow} \Delta h_{lm} \quad (2.87)$$

where $X' = 1 / m_a$

$$Y' = -b / (m_w C_{pw})$$

$$b = (h_{sw2} - h_{sw1}) / (t_{w2} - t_{w1})$$

In the analysis 'b' was assumed as constant since over a small range of tube fluid temperature variation this is valid.

$$\Delta h_{lm} = \frac{(h_{a2} - h_{sw2}) - (h_{a3} - h_{sw1})}{\ln(h_{a2} - h_{sw2}) / (h_{a3} - h_{sw1})} \quad (2.88)$$

Where h_{a2} = air enthalpy at interface, kJ/kg or Btu/lbm

h_{a3} = outlet air enthalpy, kJ/kg or Btu/lbm

h_{sw1} = tube surface enthalpy at tube fluid inlet, kJ/kg or Btu/lbm

h_{sw2} = tube surface enthalpy at tube fluid outlet, kJ/kg or Btu/lbm

U_{ow} = Pseudo overall heat transfer coefficient based on air enthalpy
difference, kW-m²-kJ/kg or Btu/hr-ft²-Btu/lba

A_{ow} = area, m² or ft²

Δh_{lm} = log mean enthalpy difference, kJ/kg or Btu/lbm

t_{w1} = inlet tube fluid temperature, °C or °F

Solving the above system,

$$h_{a3} = K_3 h_{a2} + K_4 h_{sw1} \quad (2.89)$$

$$h_{sw2} = K_5 h_{sw1} + K_6 h_{a2} \quad (2.90)$$

where $K_3 = (X'+Y')/W'$

$$K_4 = X'(Z'-1)$$

$$K_5 = Z'(X'+Y')/W'$$

$$K_6 = Y'(1-Z')/W'$$

$$Z' = \exp\{U_{ow} A_{ow} (X'+Y')\}$$

$$W' = X'Z'+Y'$$

Coil surface temperature is computed from:

$$h_{s2} = \Phi(t_{s2}) = R_o h_{sw2} / \sum R + (1 - R_o / \sum R) h_{a2} \quad (2.91)$$

where $\sum R = b_p (R_i + R_f + R_p + R_c) + b_w R_o = 1/(U_{ow} A_{ow})$

$$R_i = 1/(h_i A_{piw})$$